

実験惑星学2: 高圧実験、地球深部の物質科学

- 地球核、軽元素の溶融
- 鉄酸化物の高圧物性
- 大型プレスによる超硬材料の生成
- 高圧技術の輸出

Table 4.3.2a Model compositions (major and heat-producing elements) of Mercury.

	Me1	Me2	Me3	Me4	Me5	
<i>Mantle + Crust</i>						
SiO ₂	40.8	45.0	47.2	43.5	43.6	36.26
TiO ₂	0.49	0.37	0.33	-	-	0.06
Al ₂ O ₃	9.6	7.2	6.4	4.7	0	1.45
Cr ₂ O ₃	-	-	3.3	-	-	0.47
MgO	40.5	40.8	33.7	47.7	54.6	17.48
FeO	0.05	0.04	3.7	0	0	-
MnO	-	-	0.06	-	-	-
CaO	8.6	6.6	5.2	4.1	1.8	-
Na ₂ O	0	0	0.08	0	0	0.25
H ₂ O	0	0	0.016	-	-	0.95
K(ppm)	0	0	69	0	0	1.01
U(ppm)	0.053	0.040	0.034	0.026	0	1.17
Th(ppm)	0.19	0.14	0.122	0.12	0	-
<i>Core</i>						
Fe	94.1	92.4	93.5 [†]	94.5	94.5	-
Ni	5.9	7.6	5.4	5.5	5.5	24.13
S	0	0	0.35	0	0	1.83
O	-	-	-	0	0	5
<i>Relative Masses</i>						
Mantle + crust	61.6	60.9	32.0	35.2	35.2	-
Core	38.4	39.1	68.0	64.8	64.8	-

[†]Also 0.25% Co, 0.57% P.

Me1: Equilibrium Condensation. **Me2:** Equilibrium Condensation modified by use of feeding zones of Weidenschilling. **Me3:** Chondrite Model (Morgan and Anders, 1980). **Me4:** Extreme "dynamically mixed" model: cosmic Al/Mg ratio; sufficient SiO₂ for anorthite, diopside, and forsterite phases in mantle; core/(mantle + crust) mass ratio satisfying mean density (section 4.5.3). **Me5:** Extreme "collisionally differentiated" model, with core/(mantle + crust) mass ratio satisfying mean density (section 4.5.3).

36.26
0.06
1.45
0.47
17.48
-
0.25
0.95
1.01
1.17
-
24.13
1.83
5

Indarch
EH

Core Formation Model

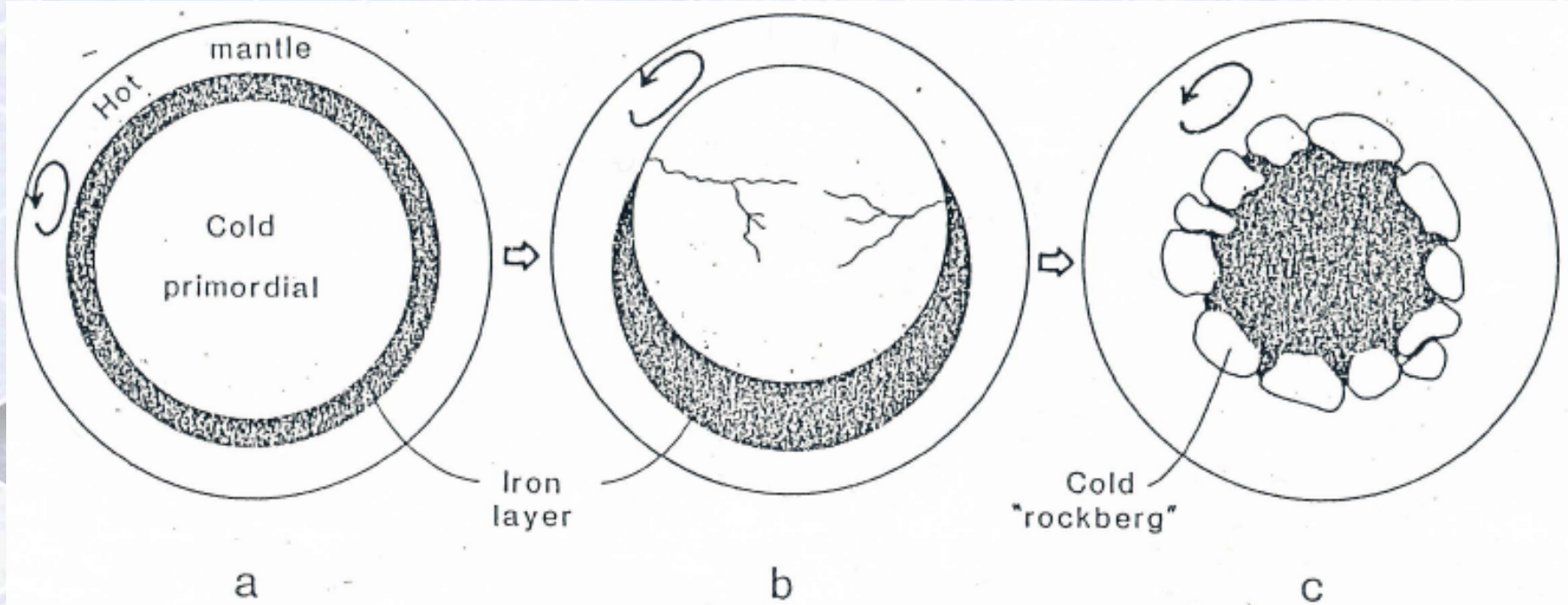


Fig. 1. Hypothetical scenario for the early stages of core formation. At this stage, the protoearth may be much smaller than the final earth. (a) A cold, undifferentiated primordial core is overlain by the denser iron that has accumulated from the partially molten mantle above. (b) A spontaneous asymmetry (23) must develop. Large, nonhydrostatic stresses on the resulting primordial core lead to deformation and even fracturing. (c) The debris from this is distributed in the form of "rockbergs" around the newly formed core. Thermal equilibration of these rockbergs with the surroundings is by thermal diffusion and takes longer than earth accretion.

Stevenson (1983)

Possible Core Materials

- Lightening elements dissolving into Fe-Ni alloy
- H (Birch, 1952; Stevenson, 1977; Fukai et al., 1982),
O (Birch, 1952; Ringwood, 1977),
S (Murthy & Hall, 1966; Brett, 1965; Usselman, 1975)
- Assessment for the Earth's outer core
- Origin of the Earth and Mercury magnetic field

Phase relations under high temperature and high pressure

- Fe-FeS, Fe-Ni-S systems up to 6 GPa (Usselman, 1975)
- Fe(Ni)-Fe(Ni)S-Fe(Ni)O system (Urakawa & Kato, 1987)
- Fe-FeO, Ni-NiO systems (Kato et al.)
- FeS hpp (Fei et al., 1997; Kusaba et al., 1997; Urakawa et al., 2004)

Mercury Pressure, density - Depth

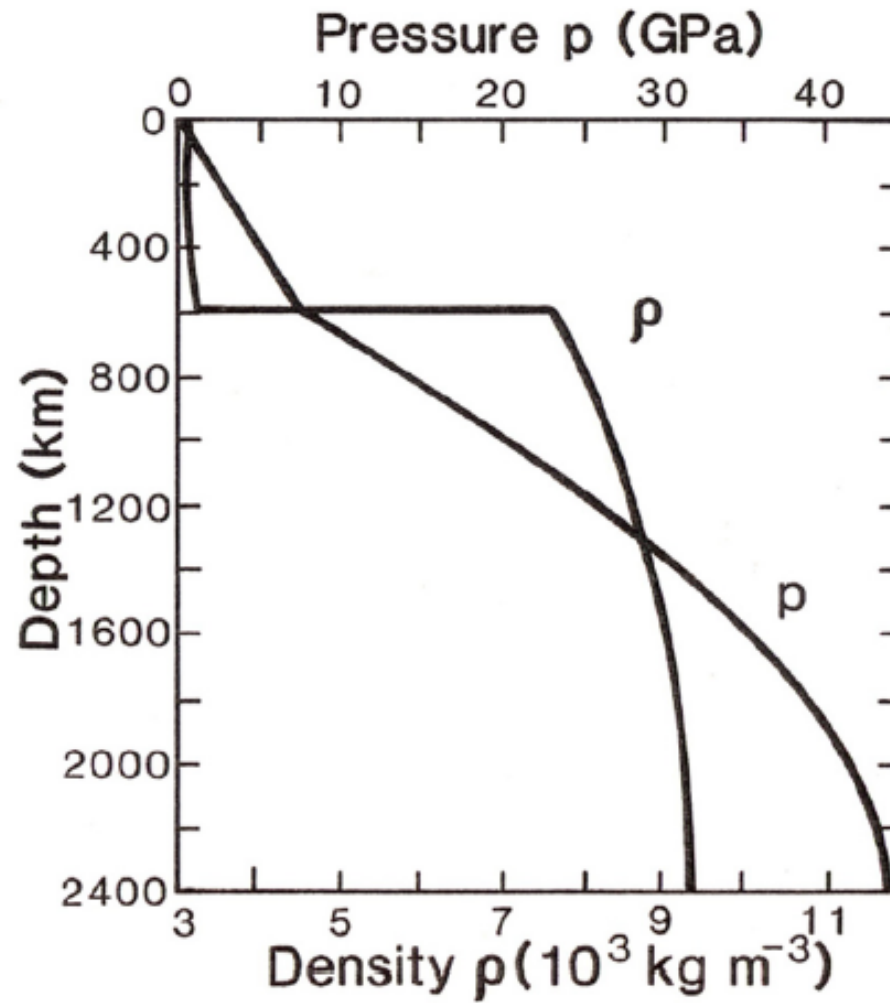
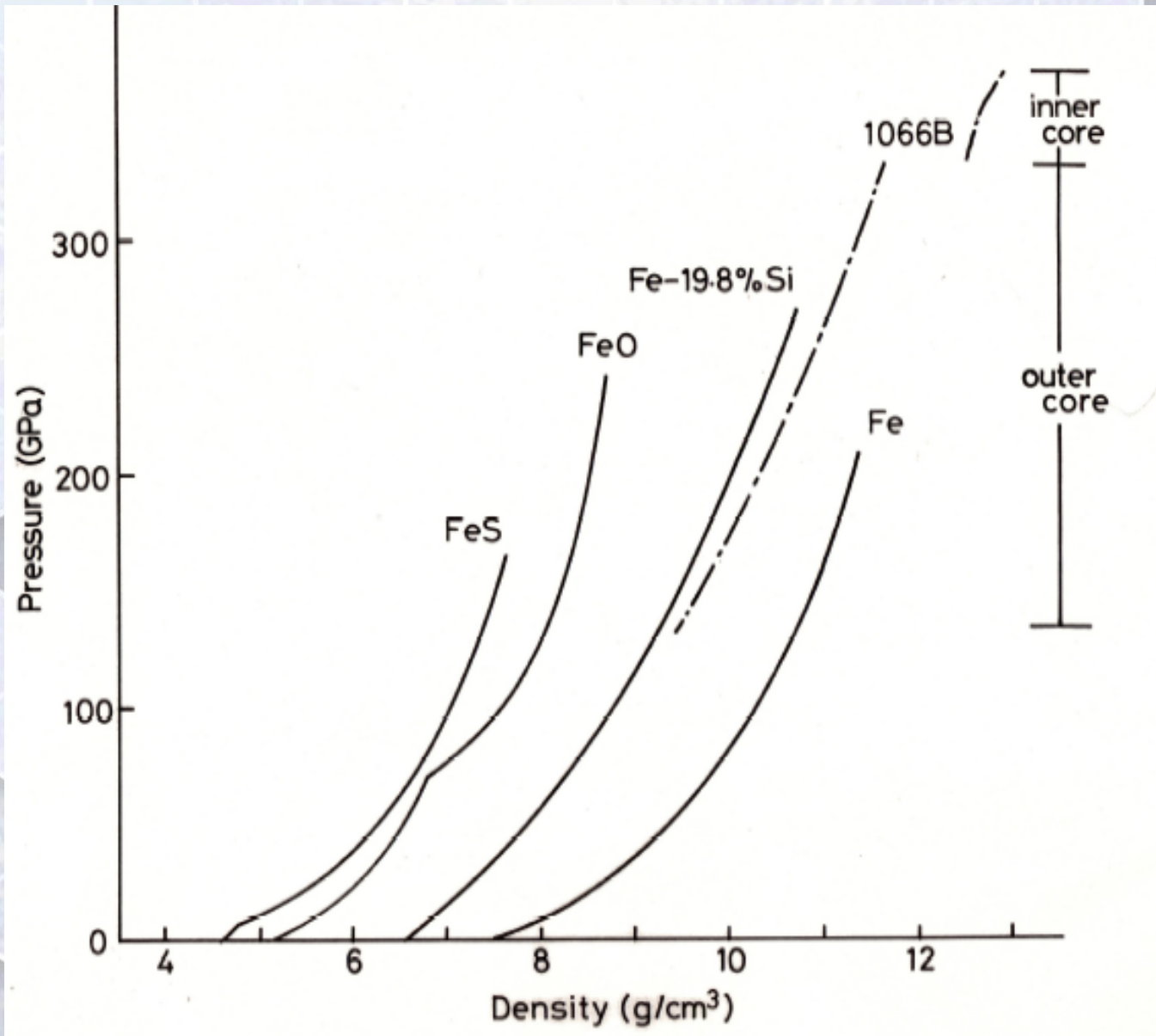


Fig. 1. Pressure p and density ρ as functions of depth in a fully differentiated Mercury model (figure after Siegfried and Solomon 1974).

Equations of state for Earth's core materials



Fe - O₂ system at
10⁵ Pa,
Levin et al.,
1964, Phase
Diagrams for
Ceramists, pp.38

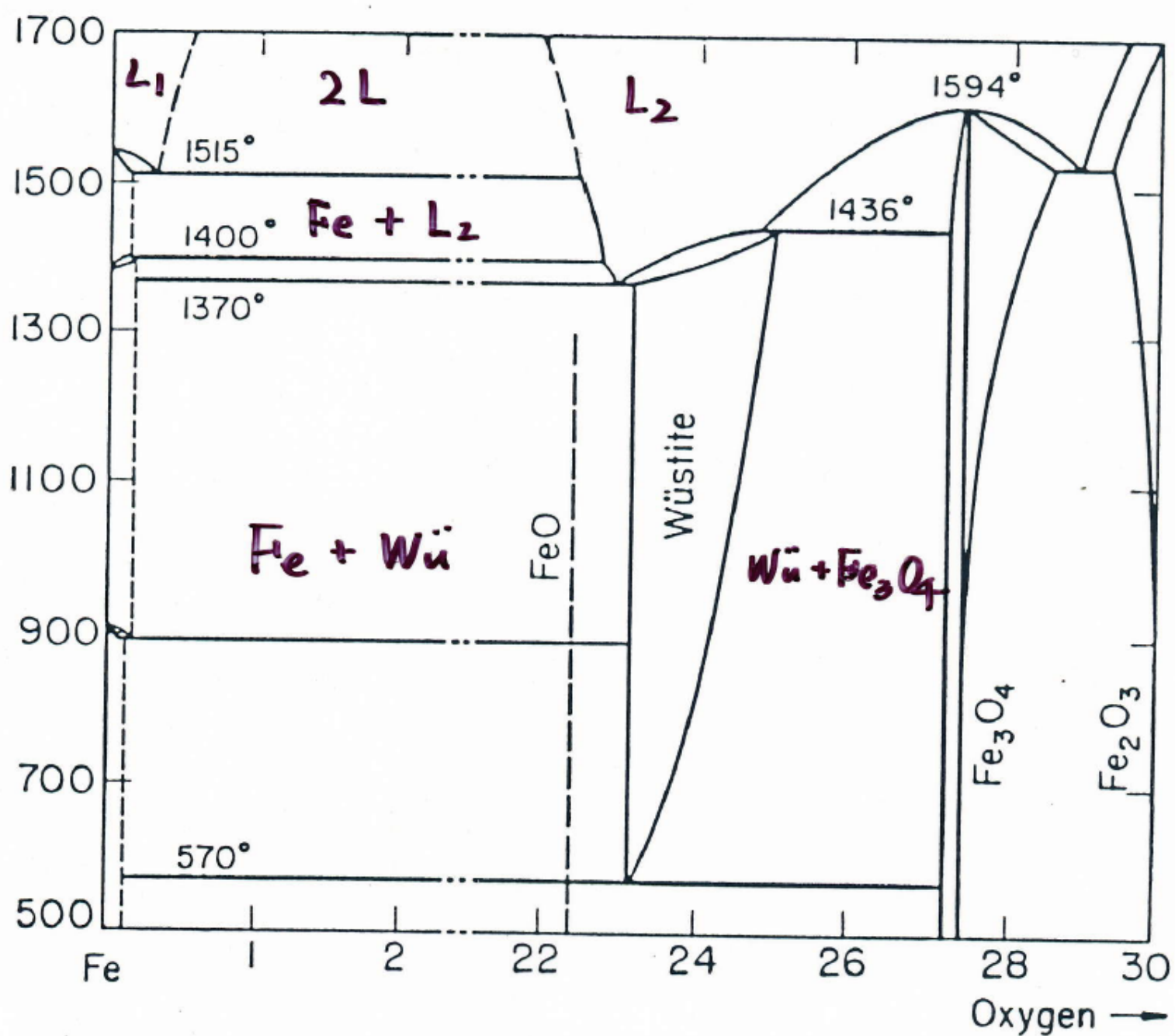
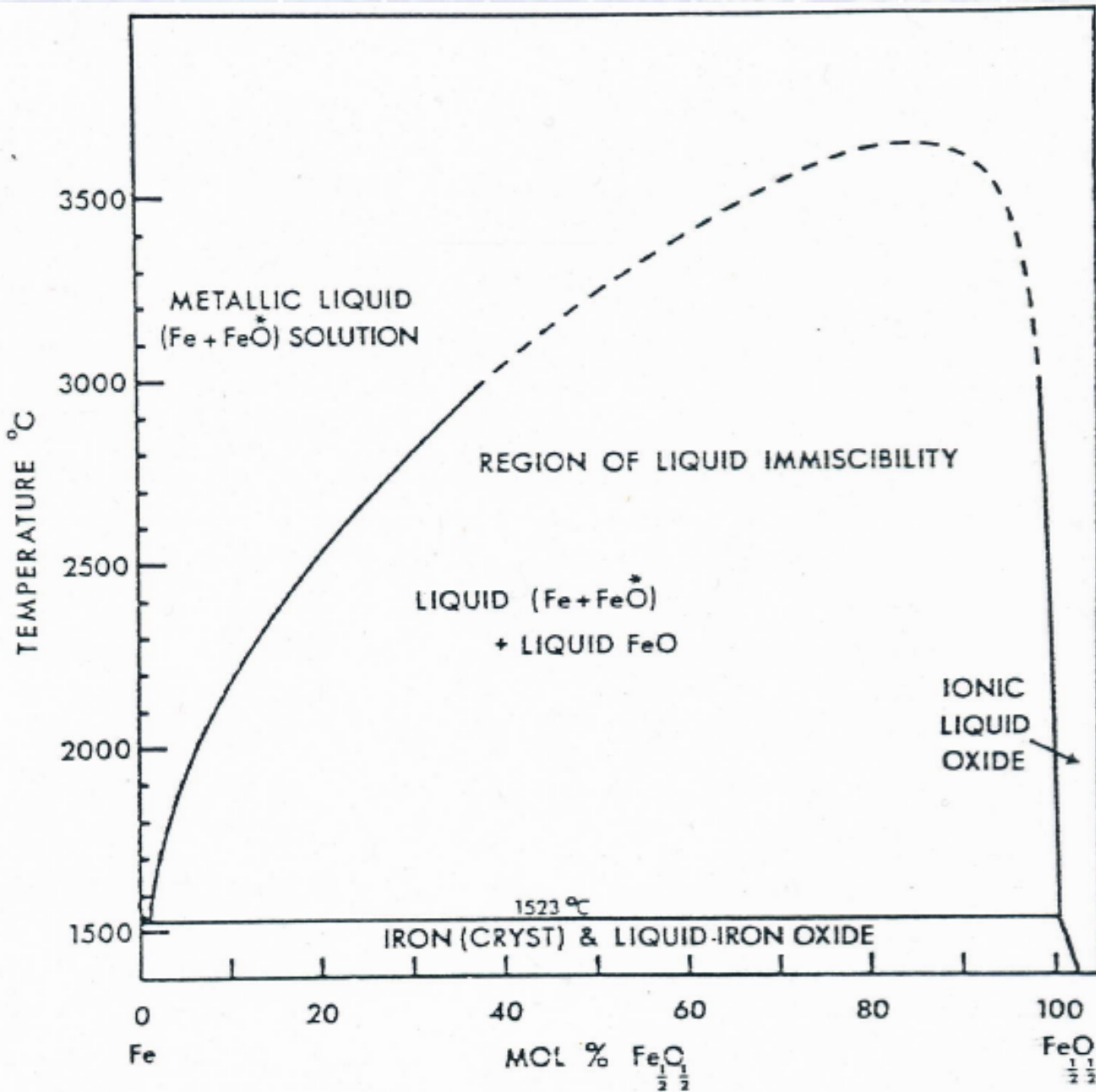


FIG. 9.—System Fe-O₂.

Liquid Immiscibility in System Fe-FeO



A.E. Ringwood, 1979,
Origin of the Earth and
Moon, pp.48.

Thermodynamics for Two Liquids Separation, Liquid Immiscibility

Fe - FeO 系における two liquid phase separation

1) 1 atm での phase diagram (Distin et al., 1971) より

理想溶液ではない

$$G^E \neq 0$$

非対称である

$$G^E \neq W_G x_1 x_2$$

2) 非対称、非理想溶液の G

$$G^L = \sum_i x_i G_i^L + \sum_i V_i^L x_i P + \sum_x R T x_i \ln x_i + \sum_{i,j} x_i x_j W_{ij}$$

$$G^L(x_1) = x_1 G_1^L + (1-x_1) G_2^L + R T \left\{ x_1 \ln x_1 + (1-x_1) \ln(1-x_1) \right\} + x_1 (1-x_1)^2 W_1 + x_1^2 (1-x_1) W_2$$

3) 熱力学的平衡 共通接線

$$G^L(x_1) - G^L(x'_1) = G^L(x'_1) - G^L(x_1)$$

$$G^L(x'_1) - G^L(x_1) = G^L(x_1) - G^L(x'_1)$$

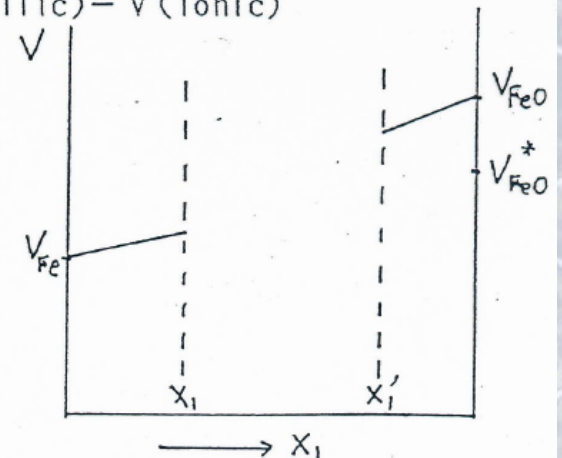
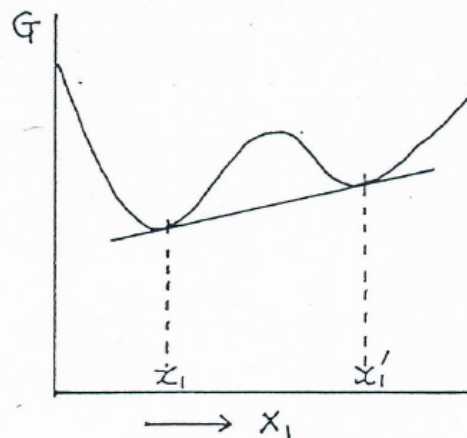
i) 1 atm での $x_1(T)$ 、 $x'_1(T)$ のデータより W_1 、 W_2 を決定。

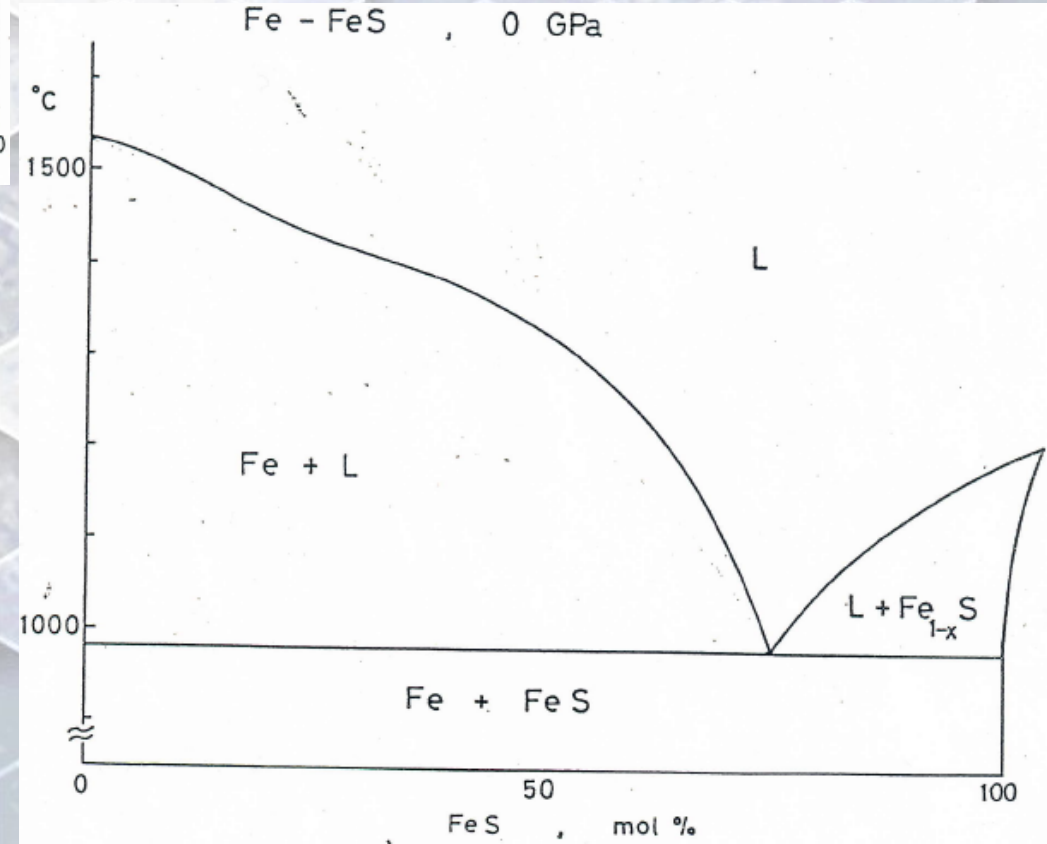
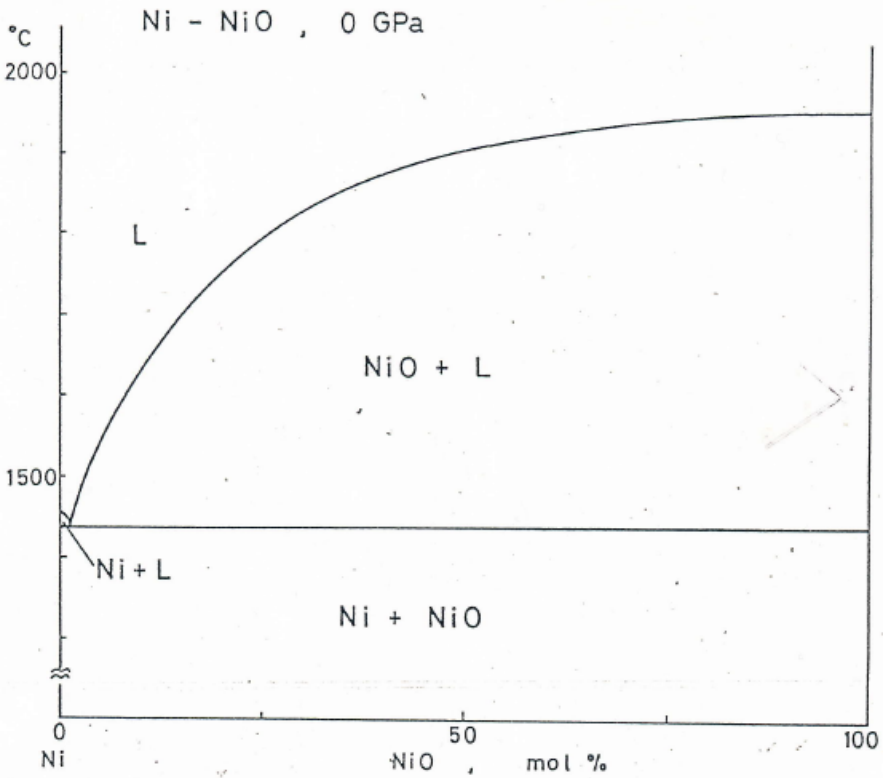
$$W = W_v + P W_v + T W_s$$

ii) P 依存性は W により決定。

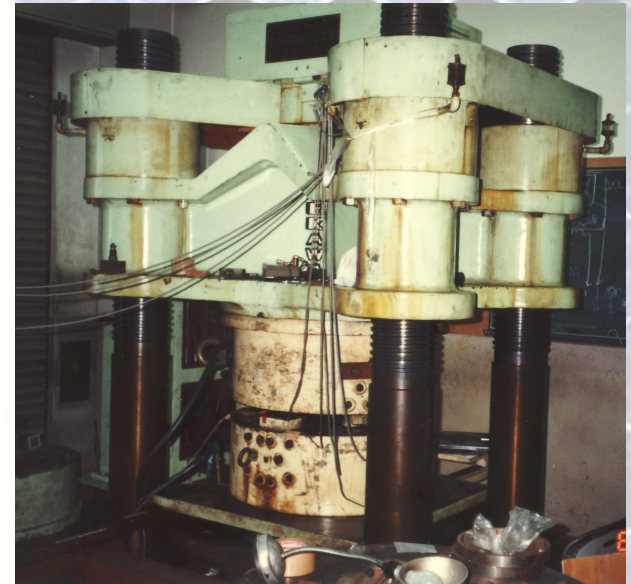
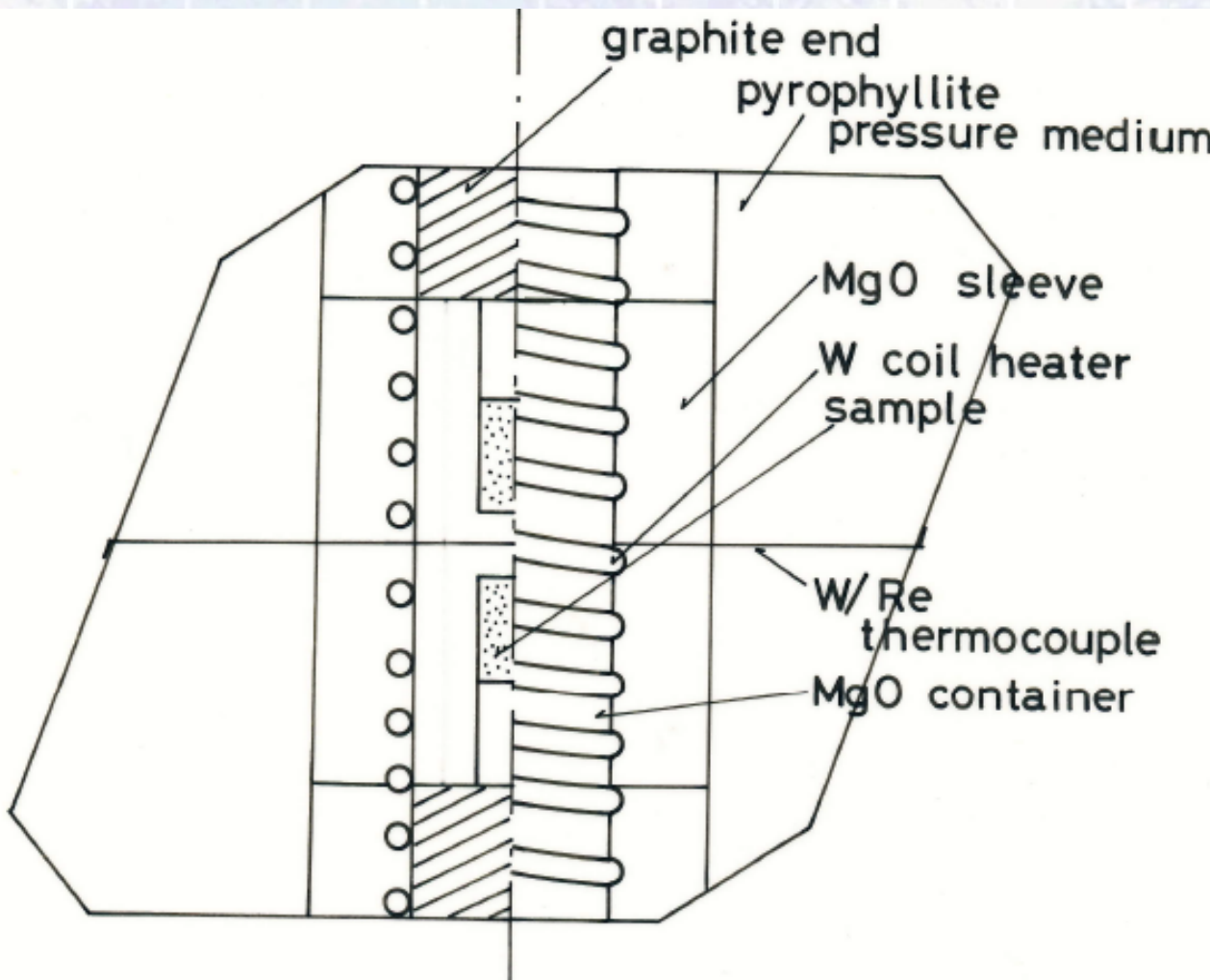
$$\text{molar volume } V = V^{id} + x_i x_j W_{ij}^V$$

$$W = V(\text{metallic}) - V(\text{ionic})$$



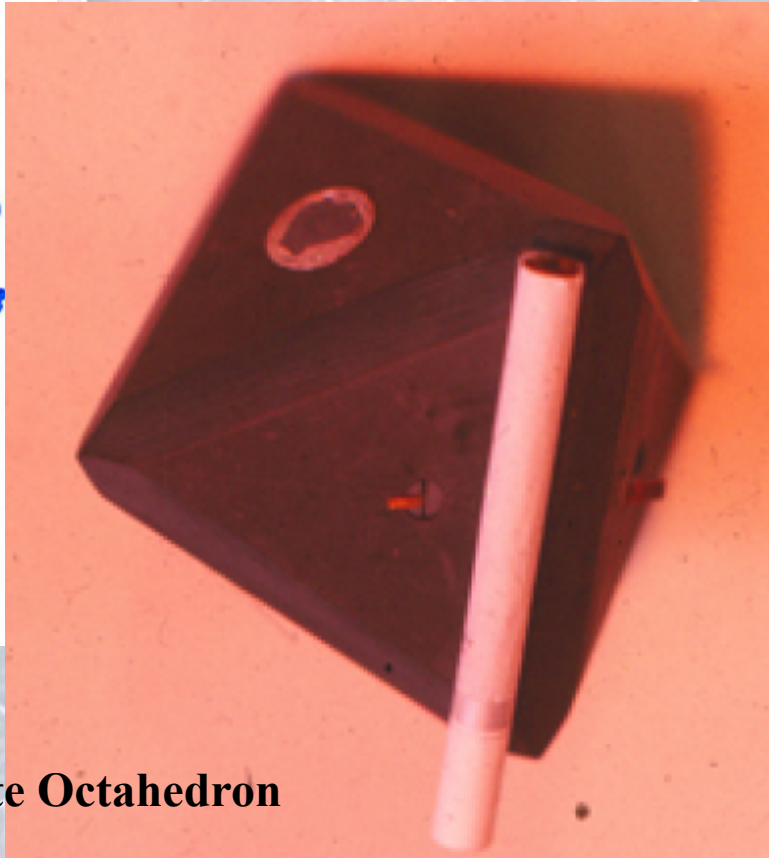
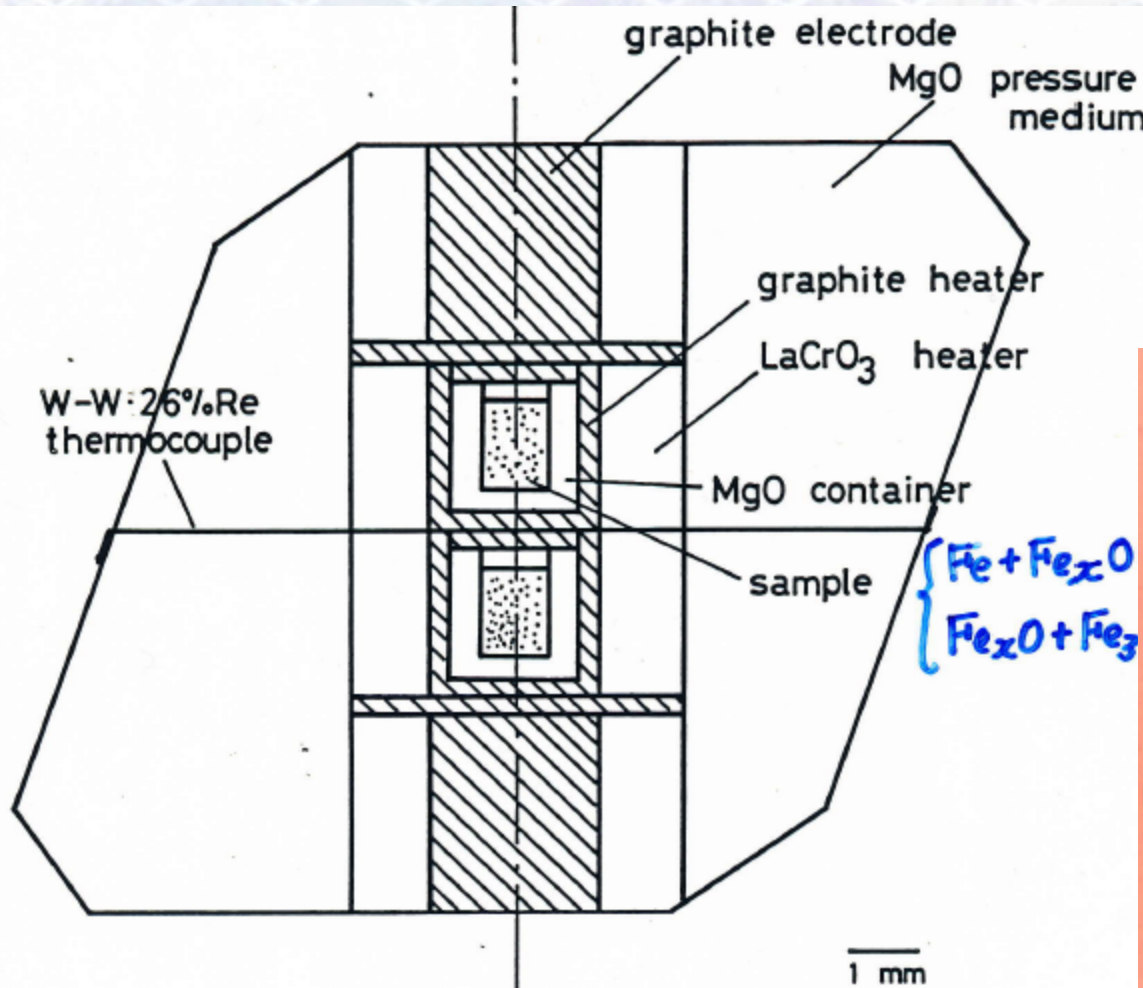


Experimental up to 15 GPa and 2500°C



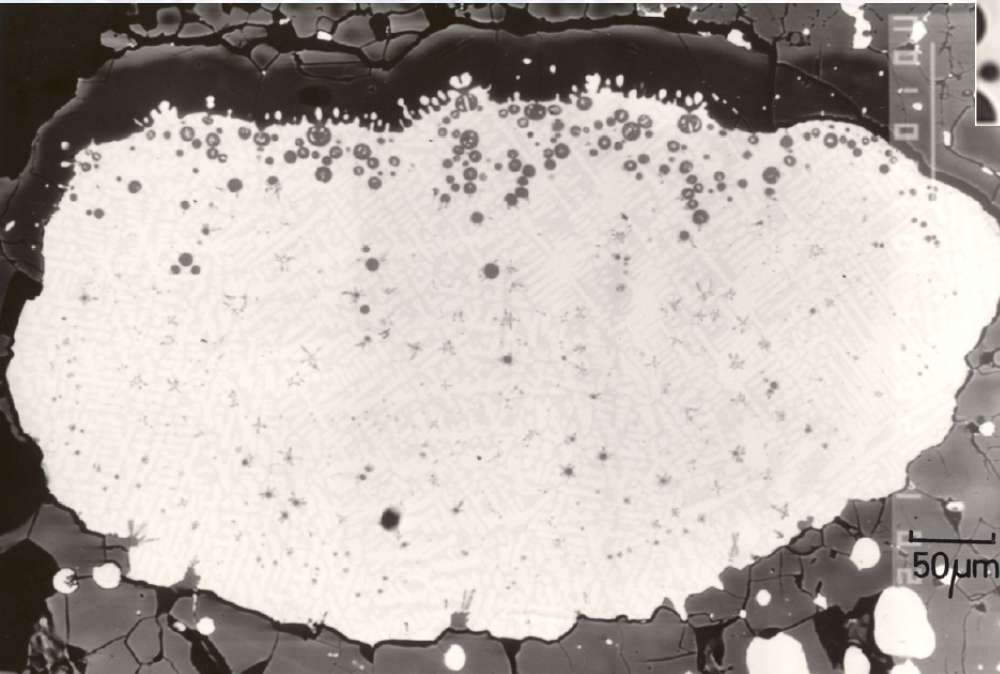
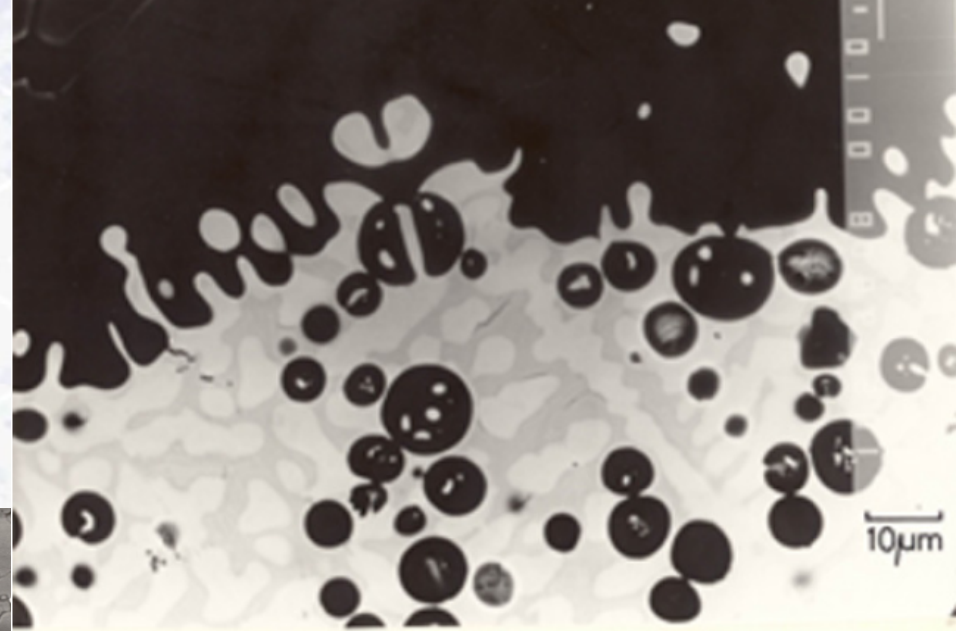
2000 ton hydraulic press

Sample Container & Pressure Transmitting Medium



60 mm Pyrophyllite Octahedron

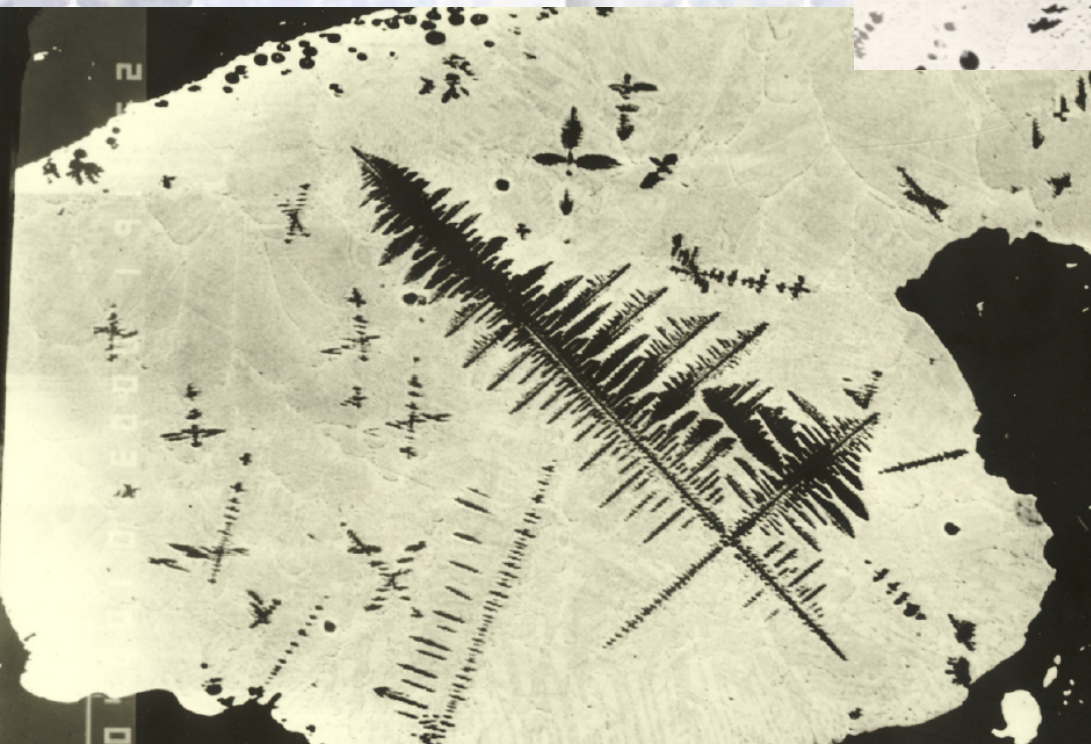
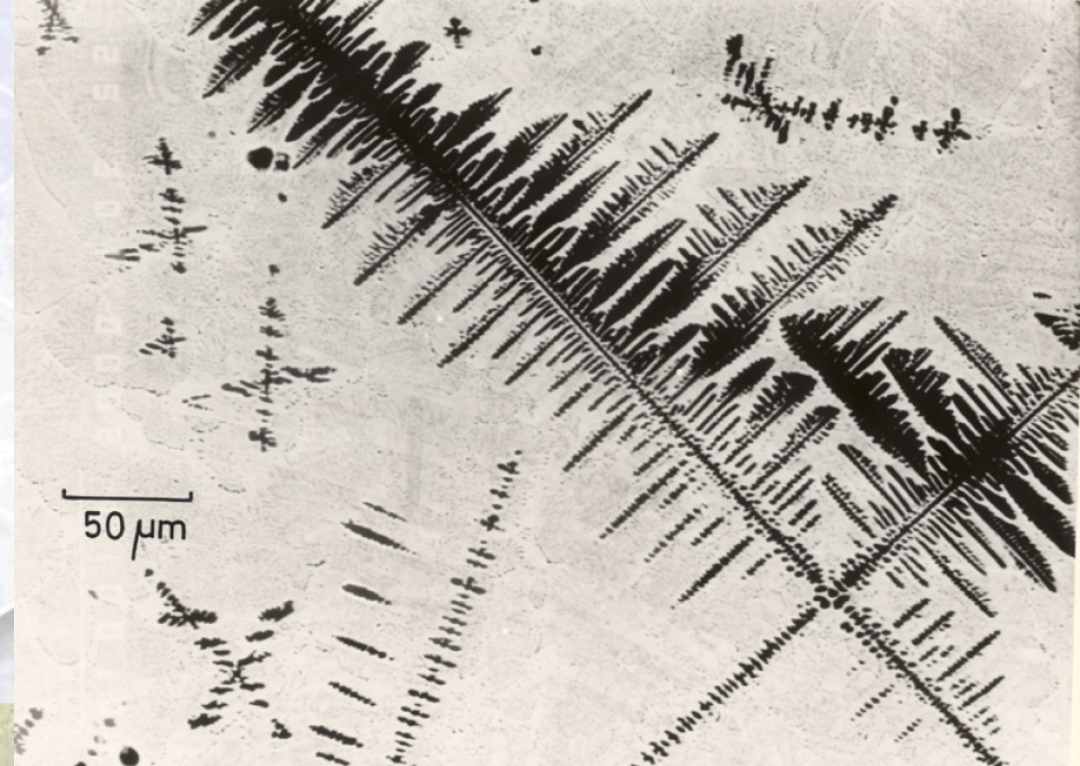
Fe-FeO, 10 GPa 2200°C

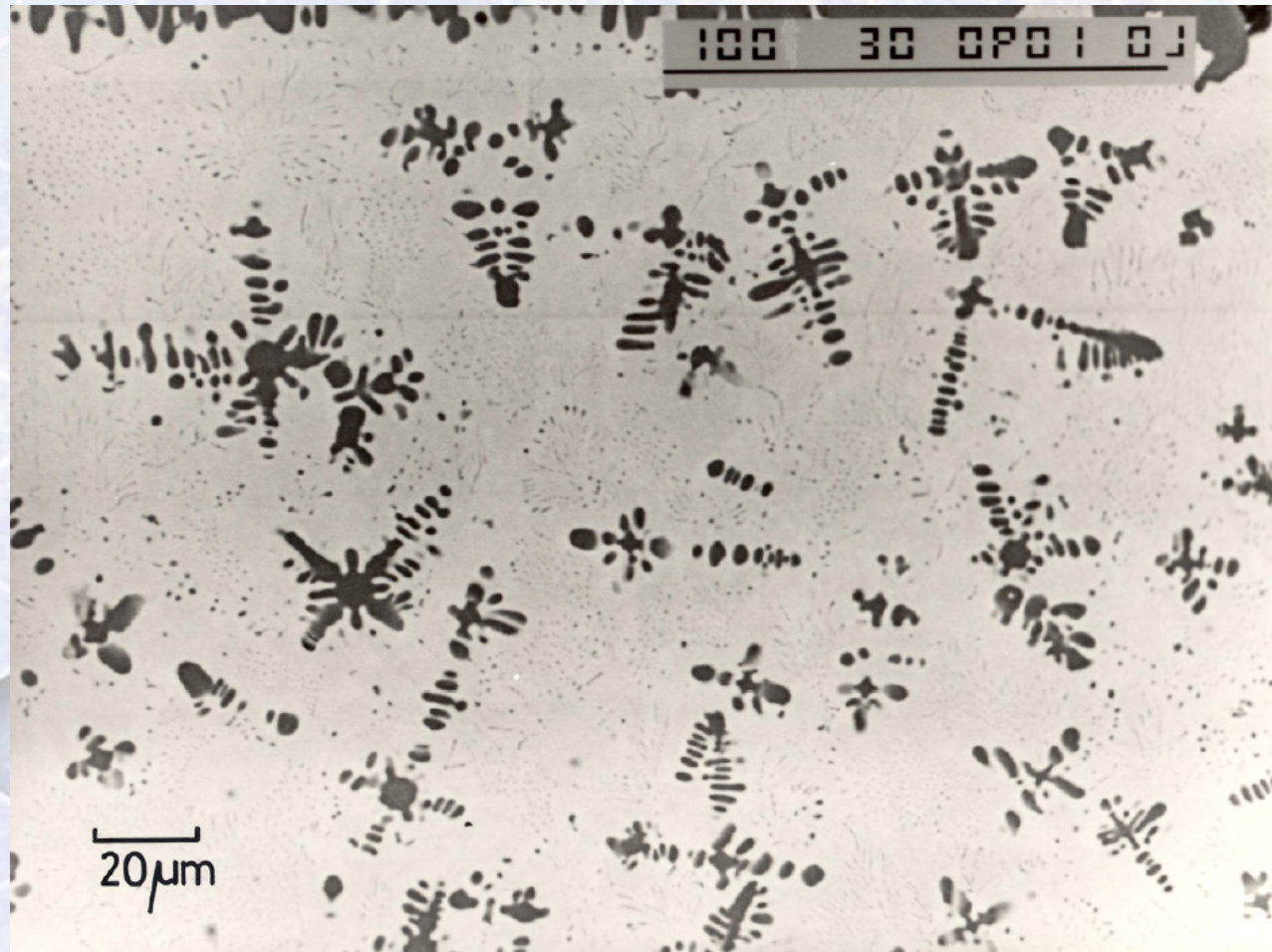


BEI

Fe-FeO, 10GP 2200°C

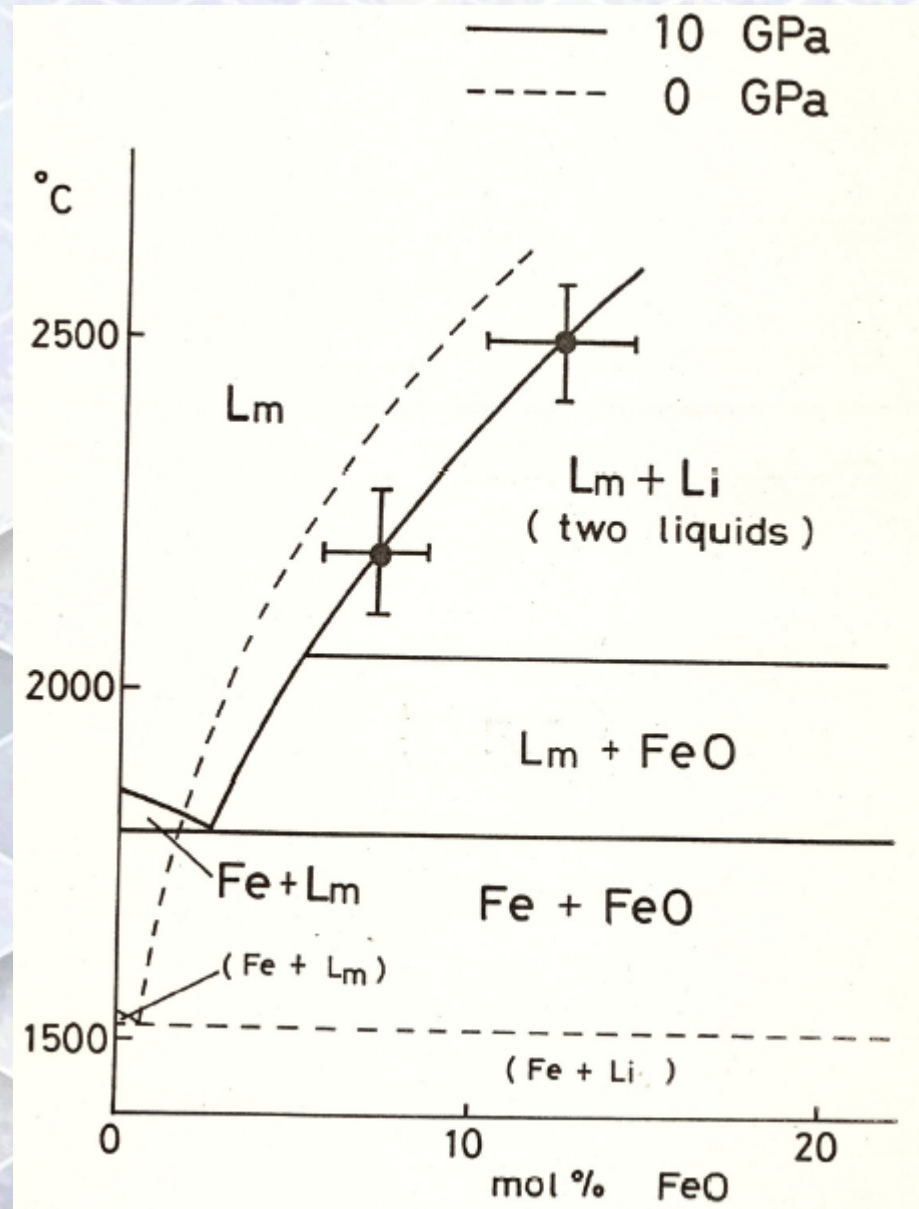
Fe-FeO, 10 GPa 2500°C



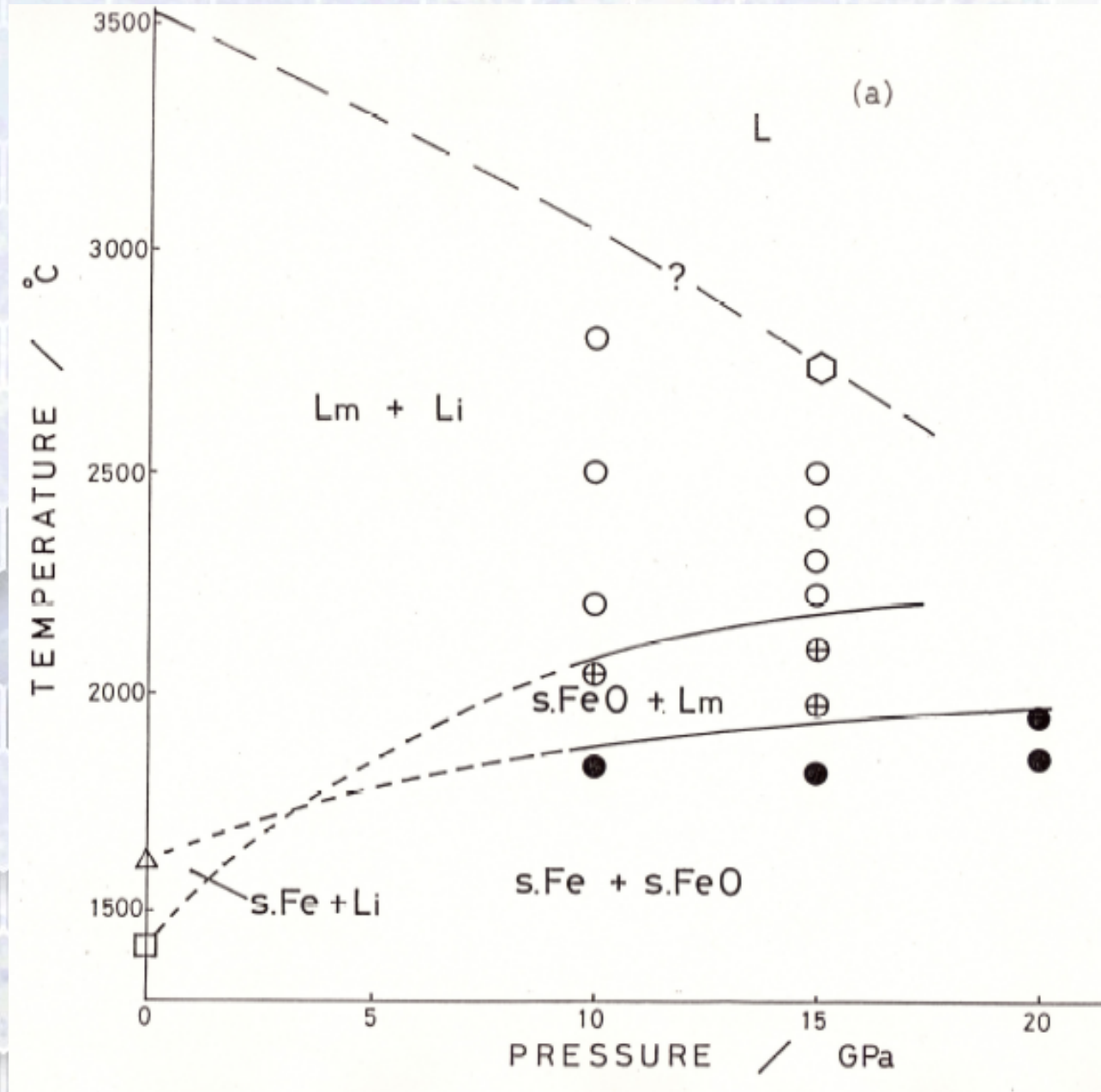


Fe-FeO, 15 GPa 1900°C

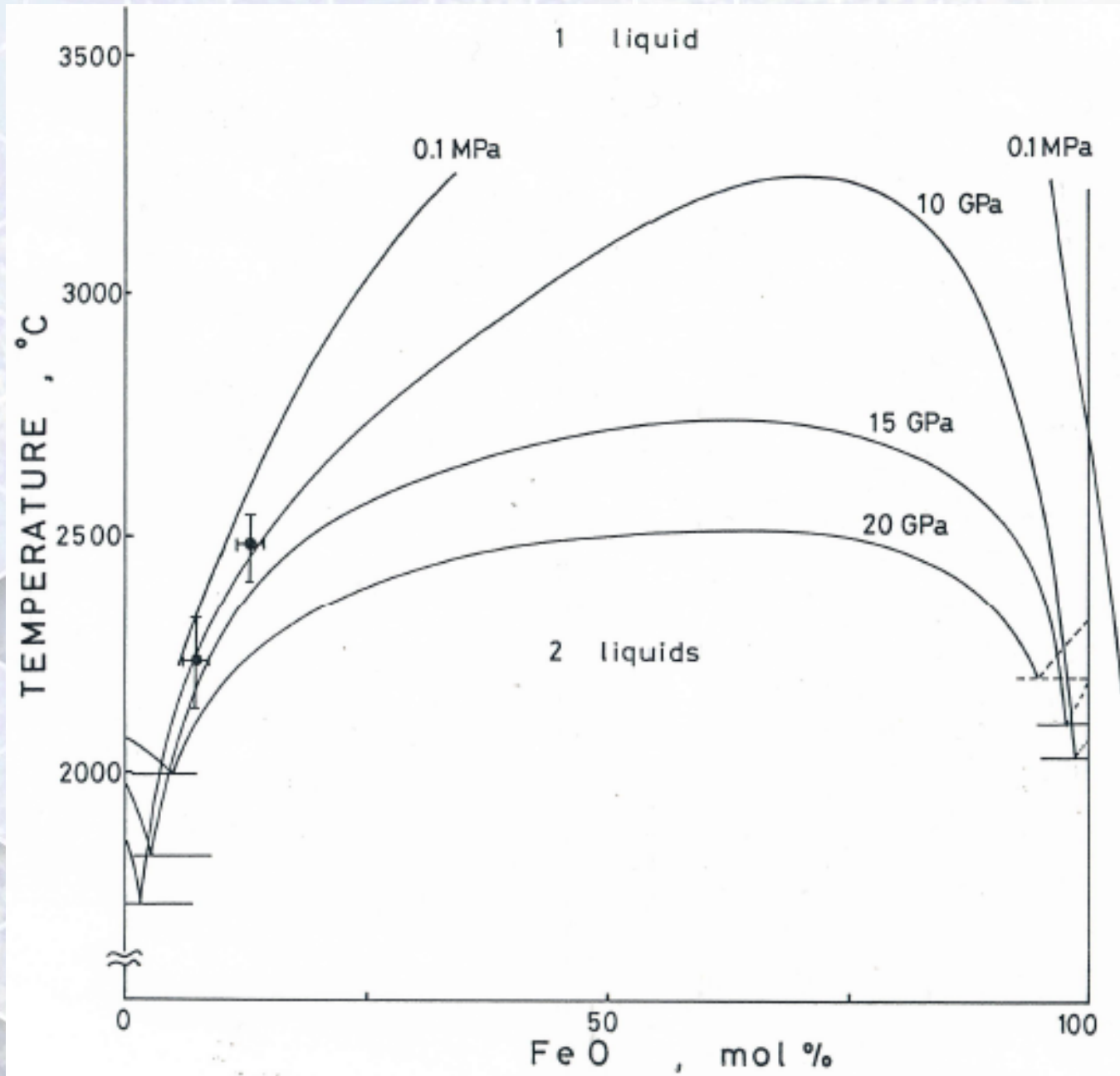
Phase Diagram of Fe-rich portion

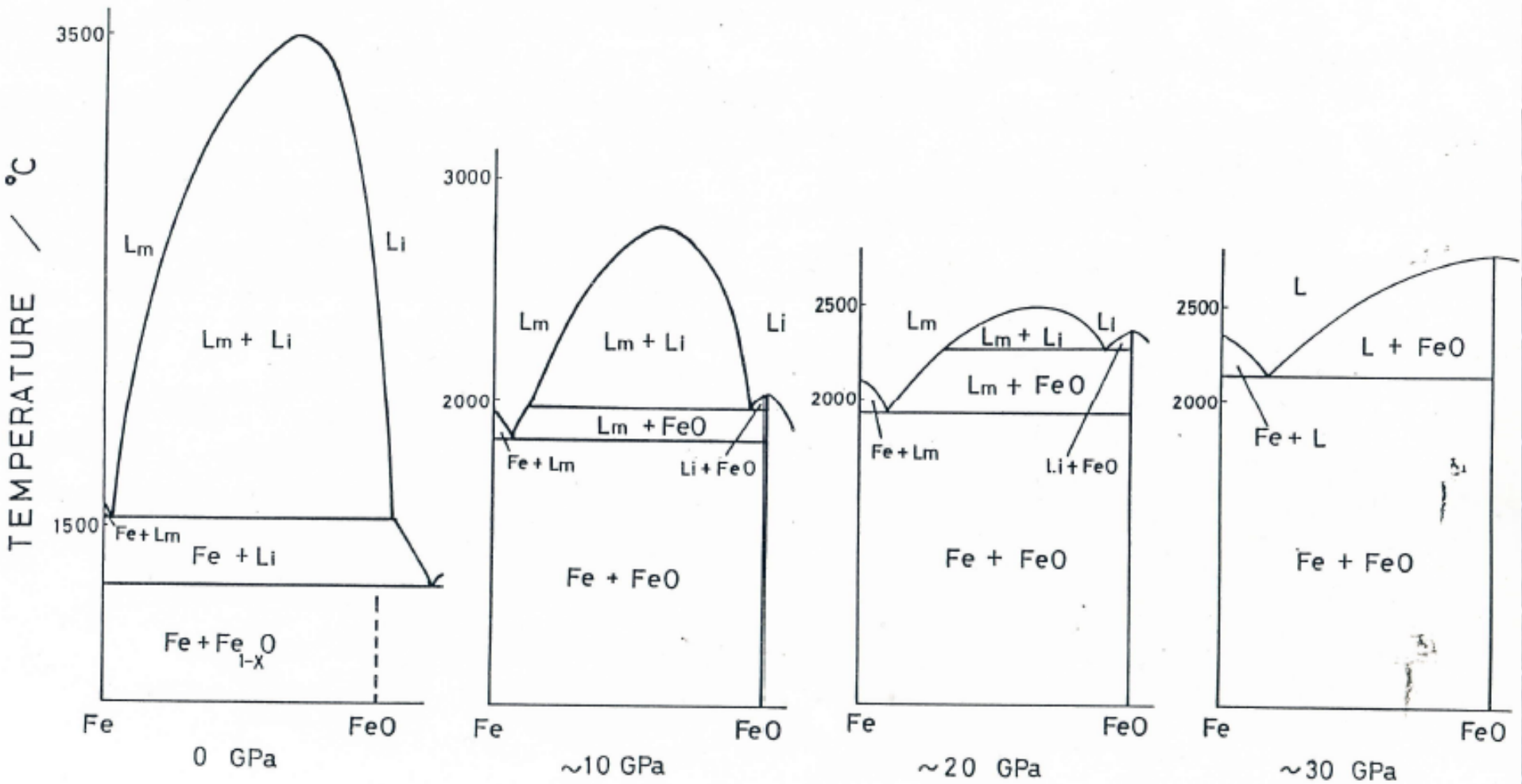


Experimental results of the system Fe-FeO



Pressure Effects on two liquid miscibility

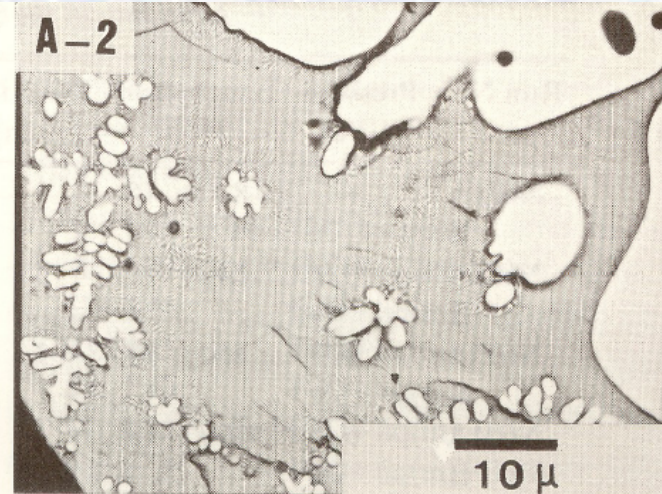
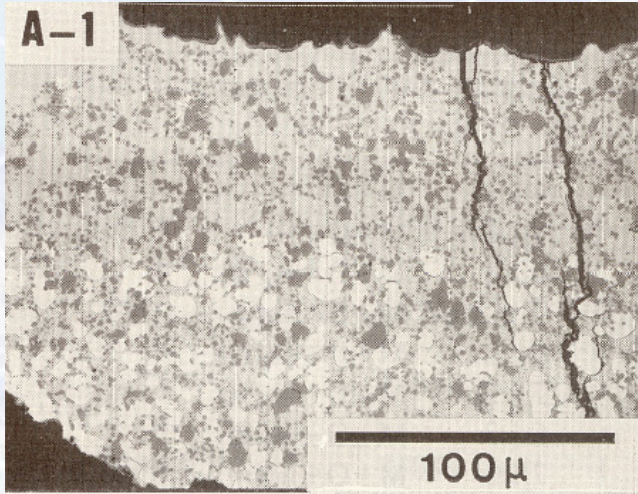




- Reduction of liquid immiscibility
- Increase oxygen solubility into liquid Fe

Fe-S-O

15 GPa
950 °C
M+O+Lm



6 GPa
940 °C
M+O+Lm

15 GPa
1500 °C
M+O+Lm

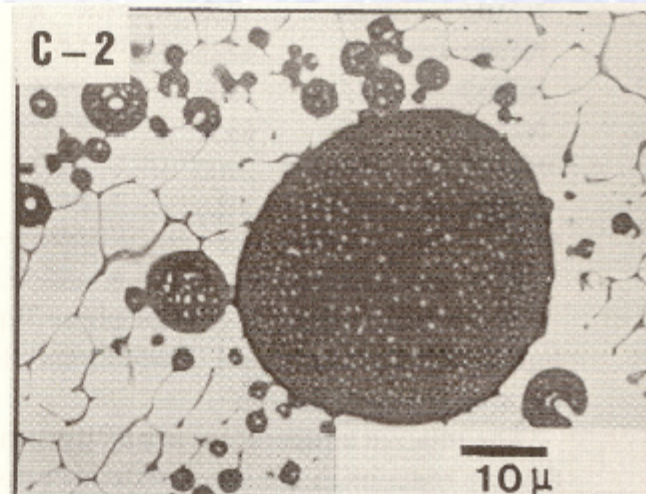
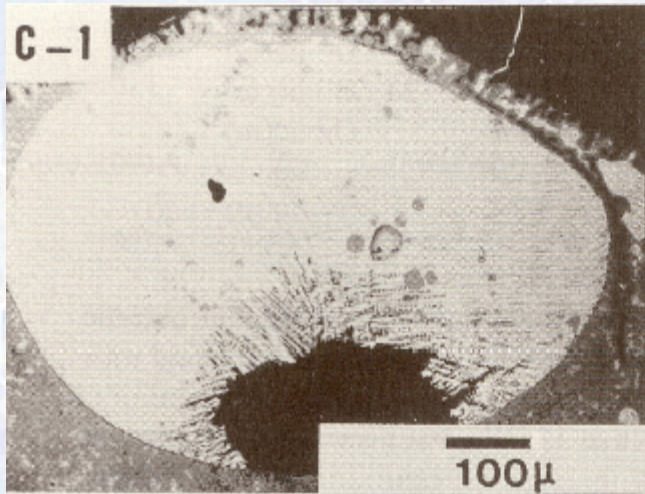


15 GPa
1500 °C
M+O+Lm

Fe-S-O

6 GP
2100°C

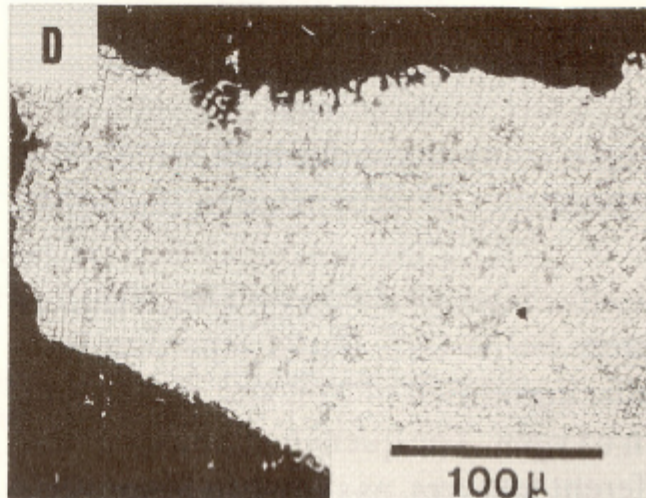
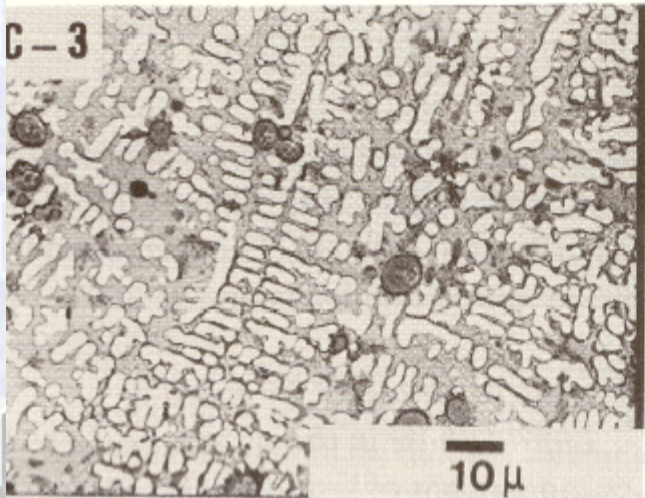
Lm+Li



6 GPa
2100°C,
Ionic droplets

6 GPa
1410°C

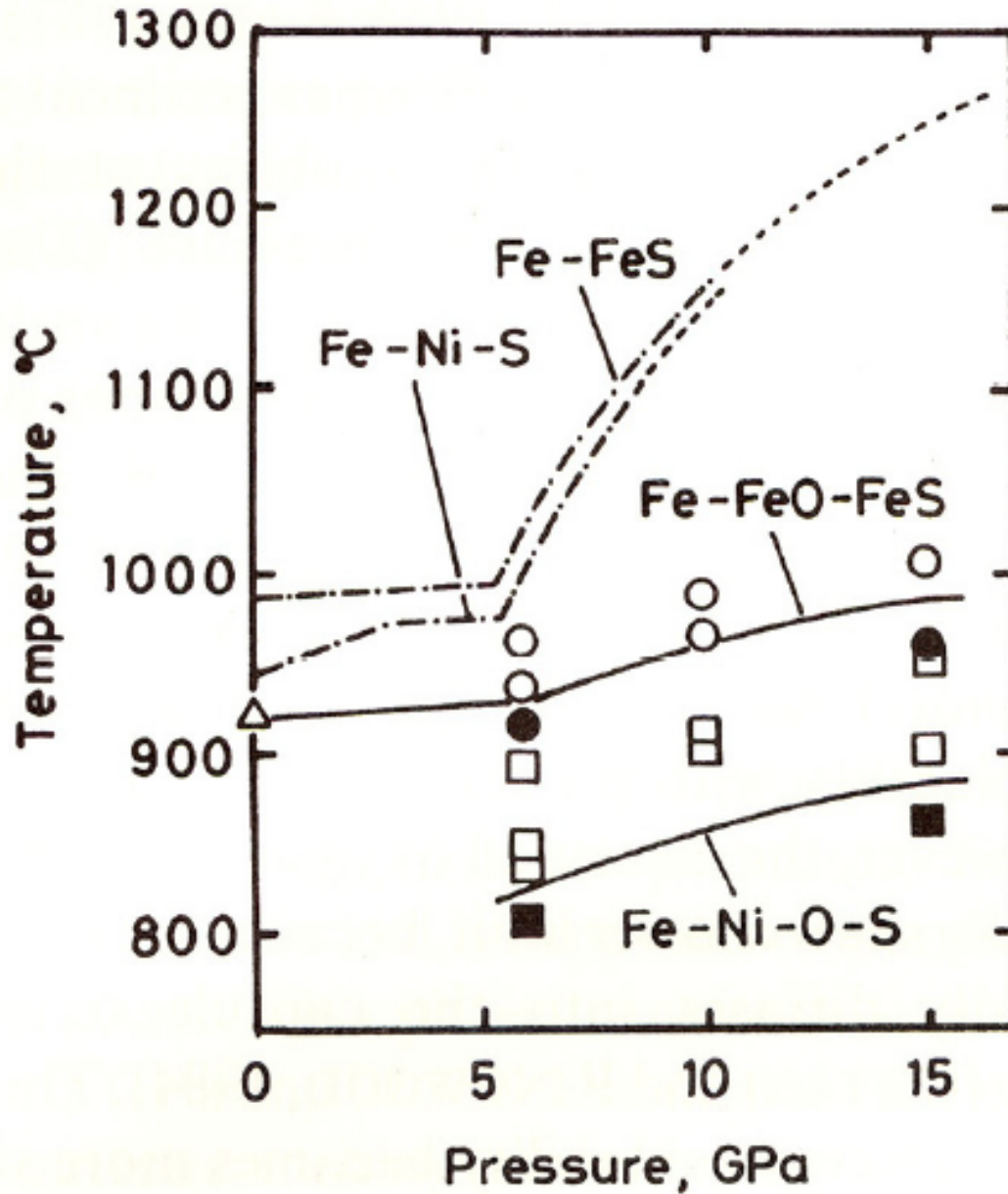
Lm+Li



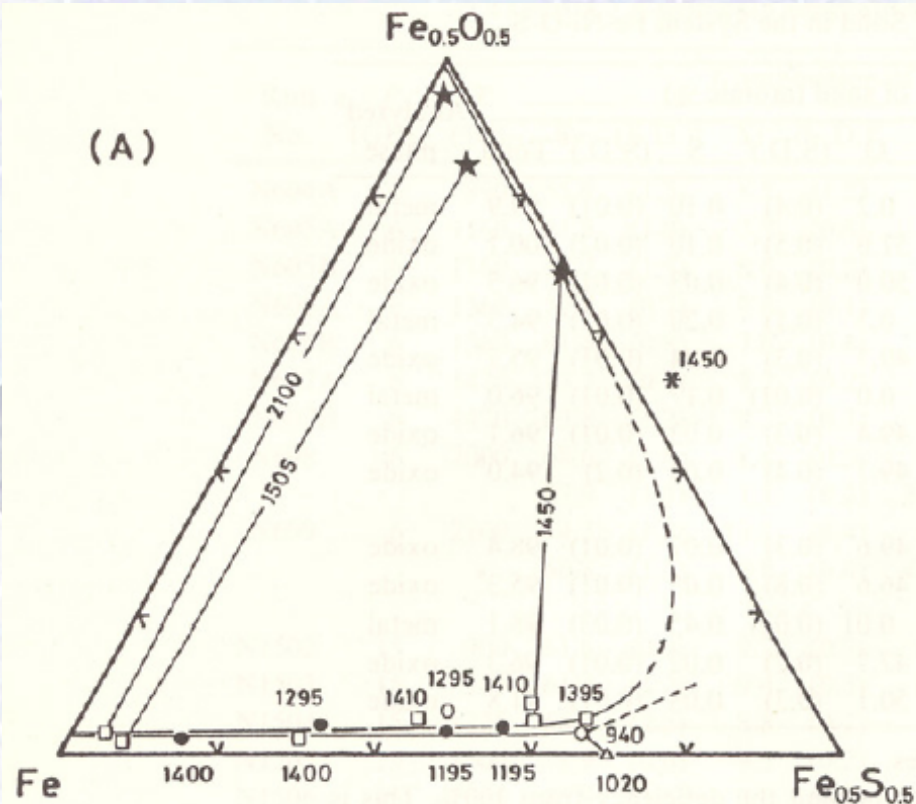
15 GPa
2000°C,
Single liq.

Urakawa & Kato, 1987

Melting curves of iron compounds

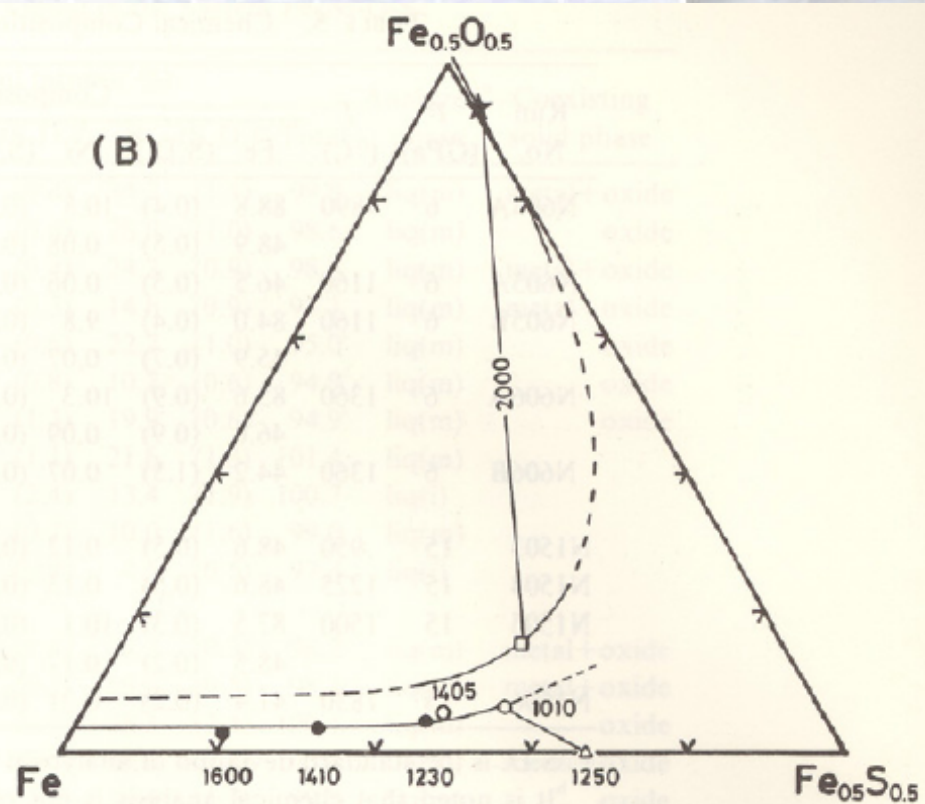


Phase relation of the system Fe-FeS-FeO



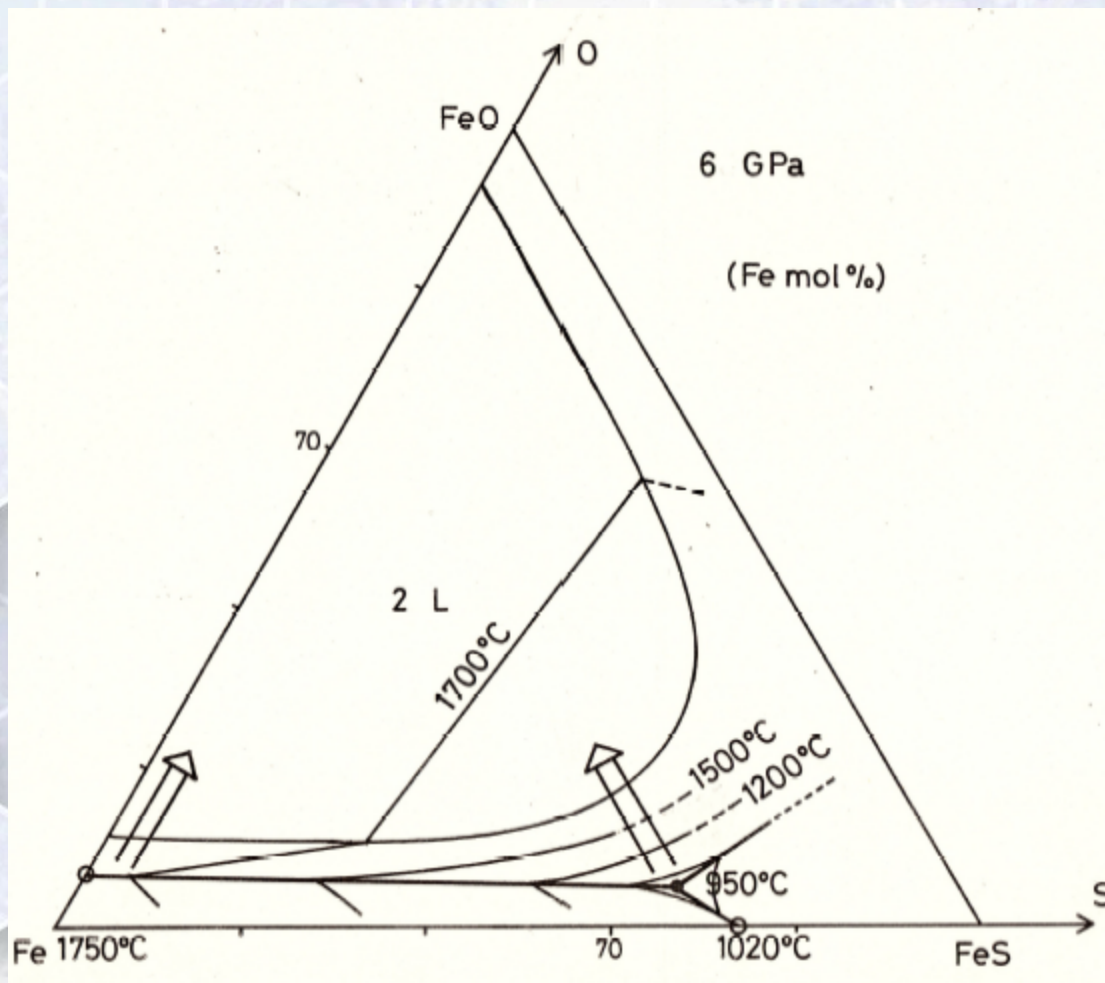
6 GPa

- ⬡ : Ternary eutectic point
- △ : Binary eutectic point
- : Liquid on cotectic line
- : Liquids coexisting with FeO

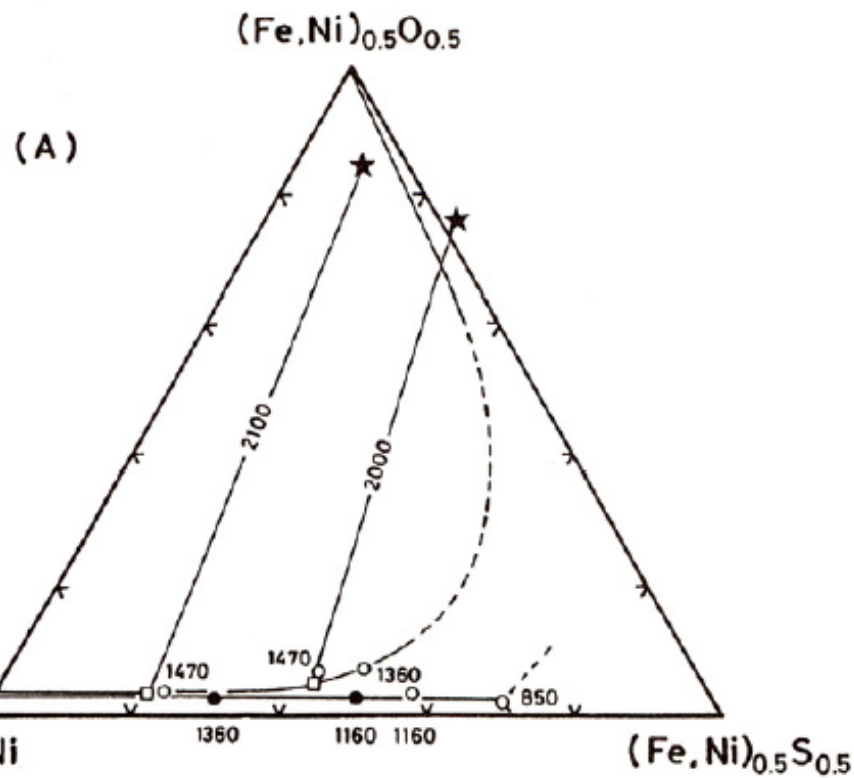


15 GPa

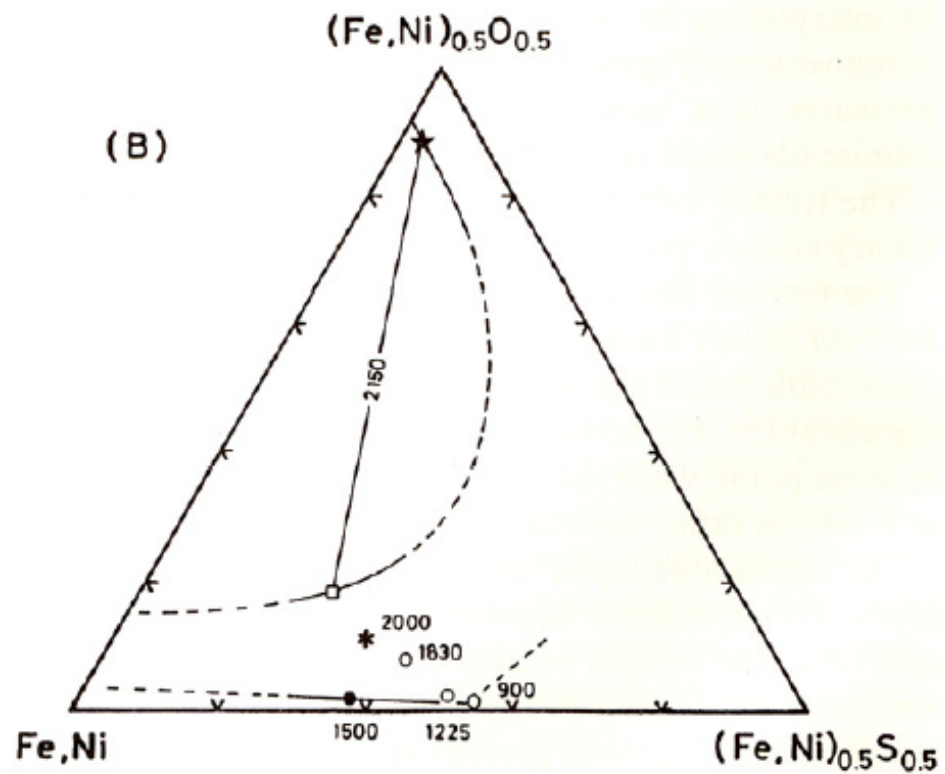
- ★ : Ionic liquid in two liquids
- : Metallic liquid in two liquids



Ni effect

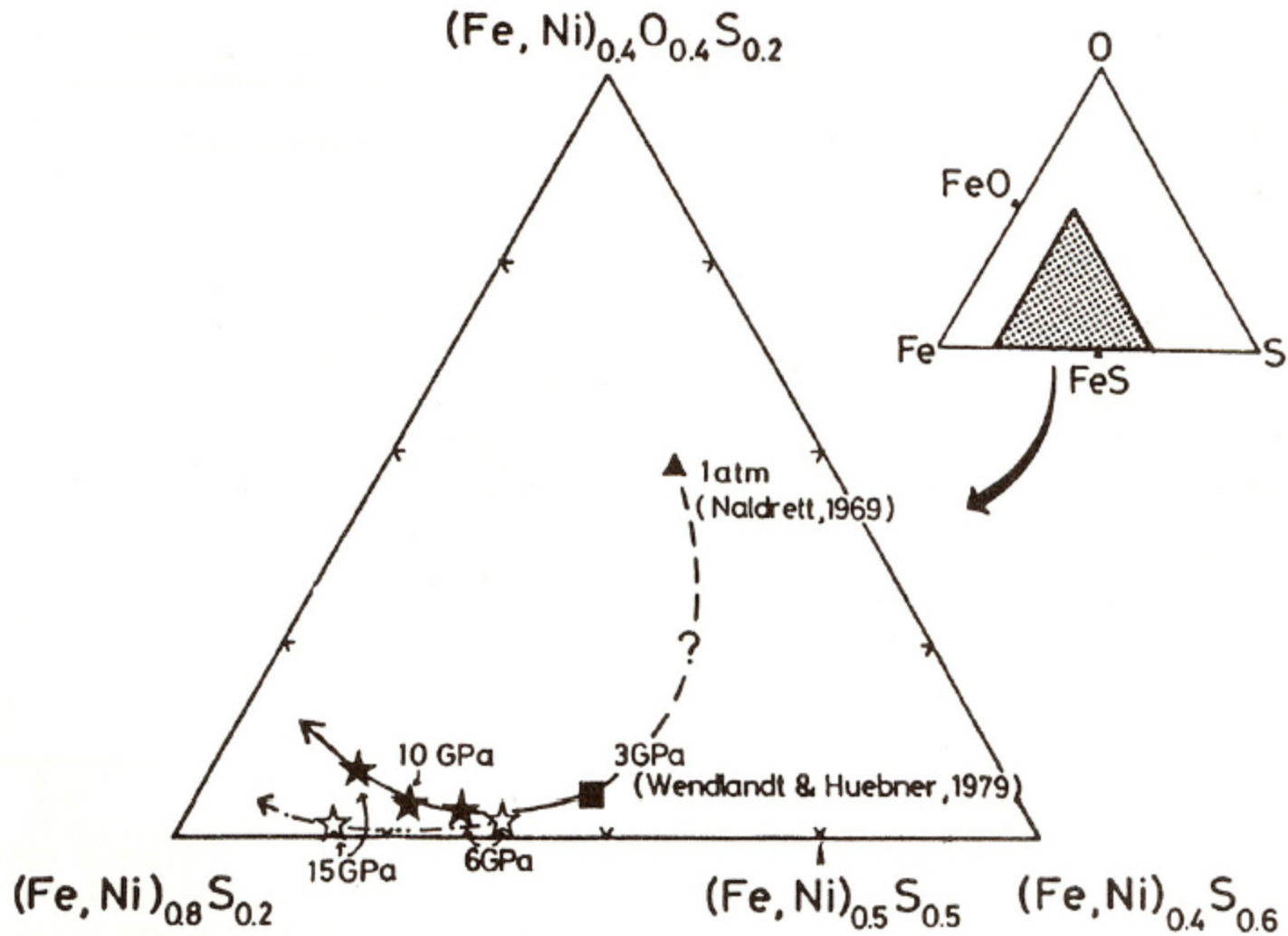


6 GPa



15 GPa

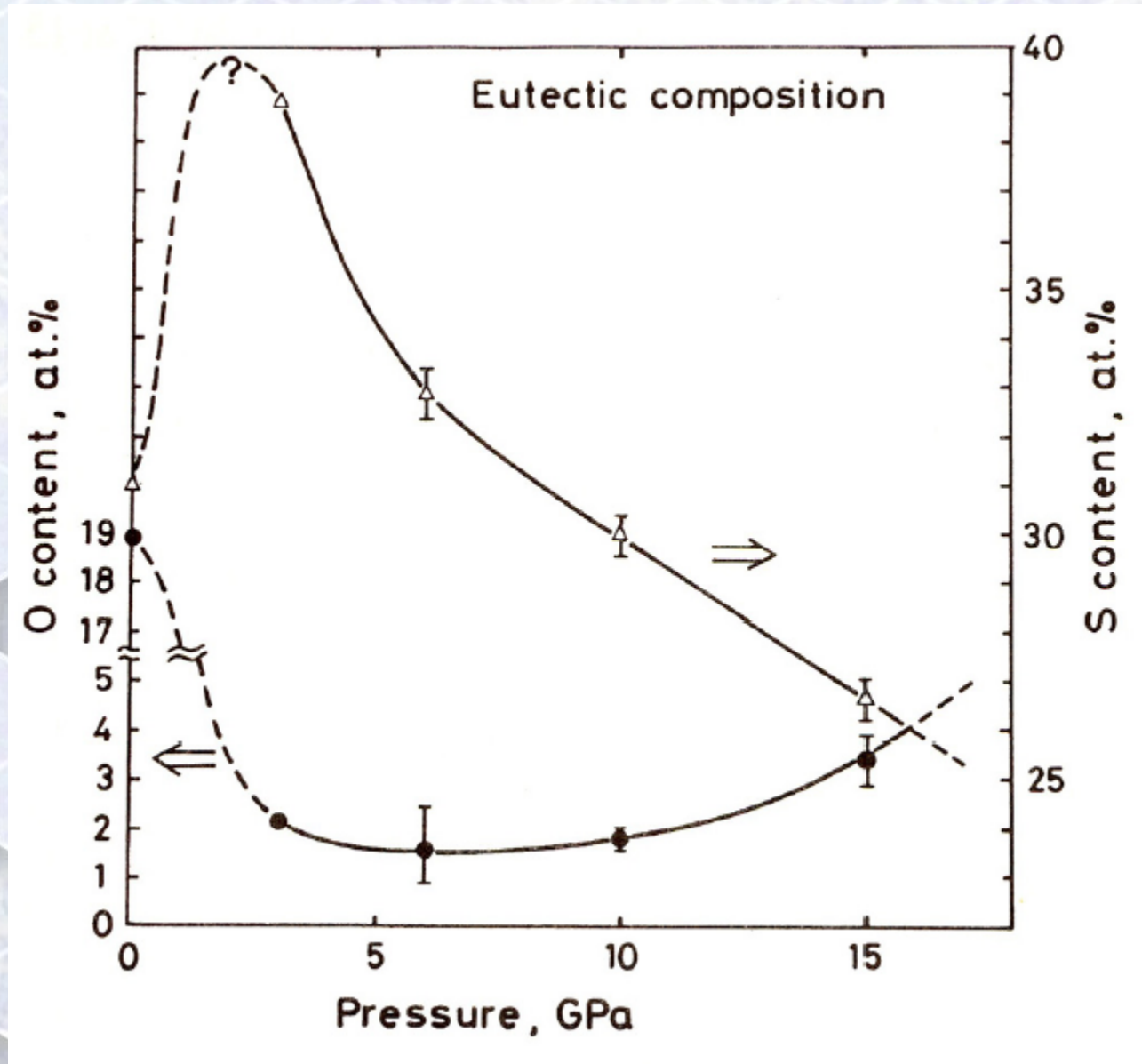
Pressure Shifts of Eutectic Composition



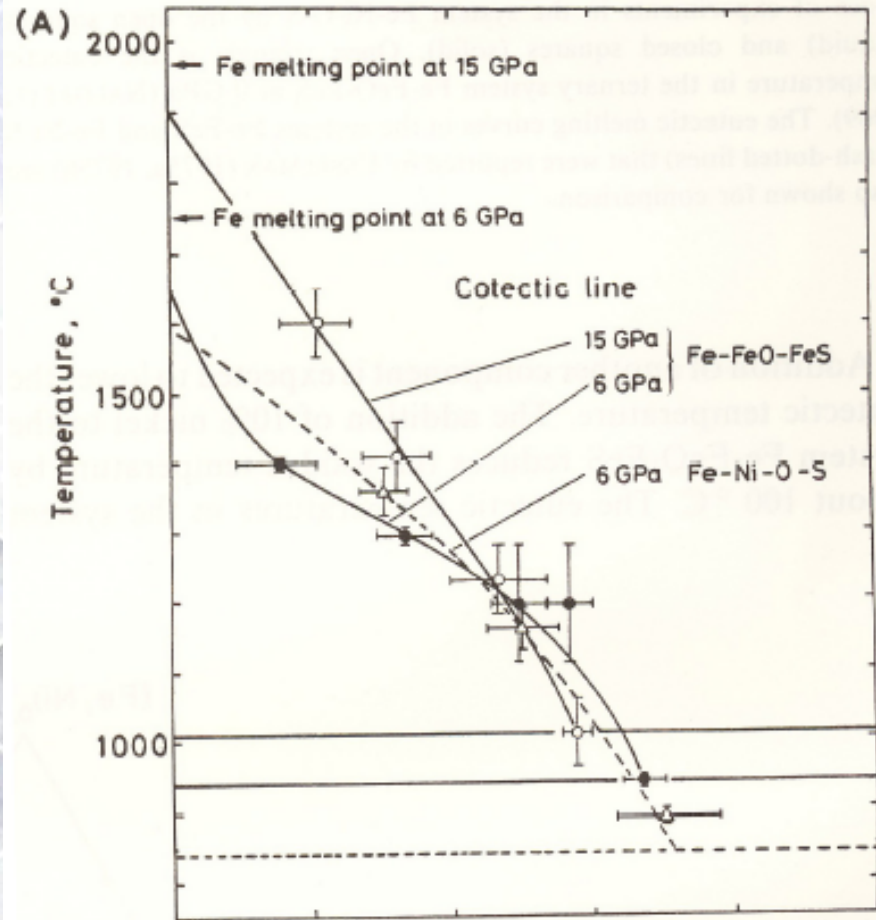
★ : Fe-S-O

☆ : Fe-Ni-O-S

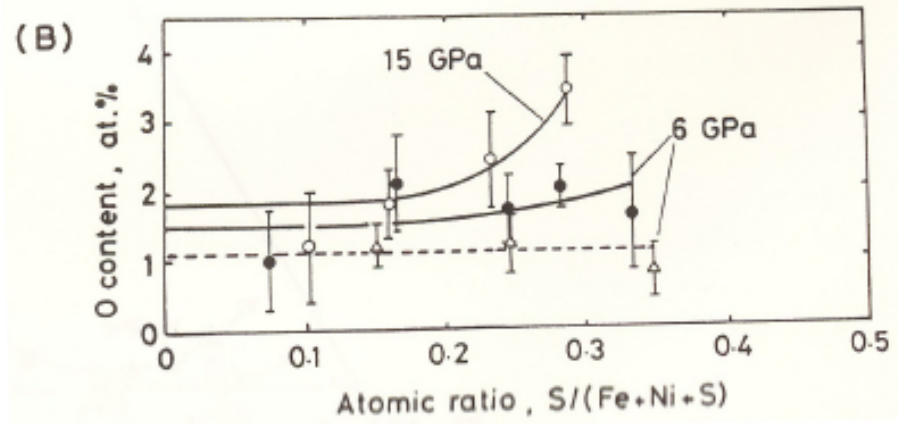
Pressure Shifts of Eutectic Composition in the System Fe-O-S



(A) Cotectic lines projected from FeO end to (Fe, Ni)- (Fe,Ni)S join

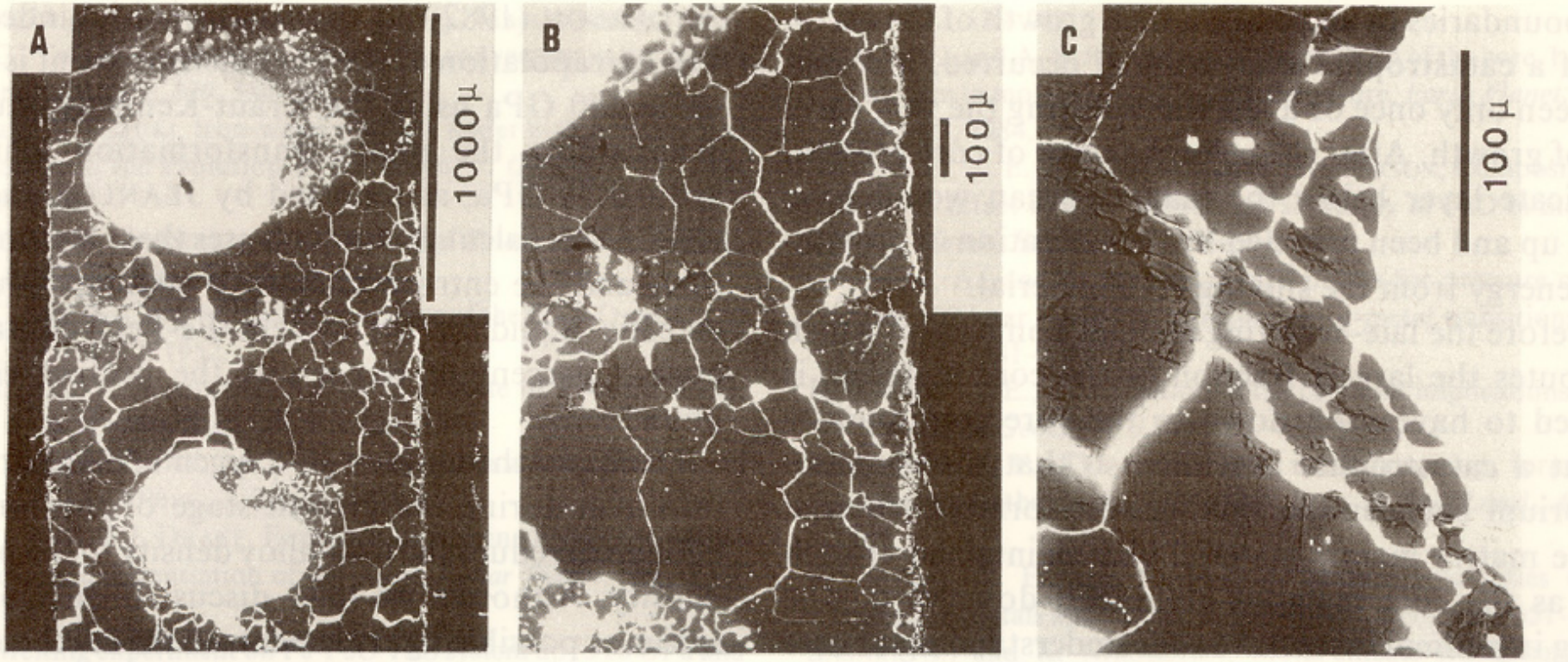


(B) Oxygen contents of cotectic liquid



Dotted lines show the case of Fe-Ni-O-S

Chemical Corrosion MgO



6 GPa, 2500 °C

New high pressure Phase

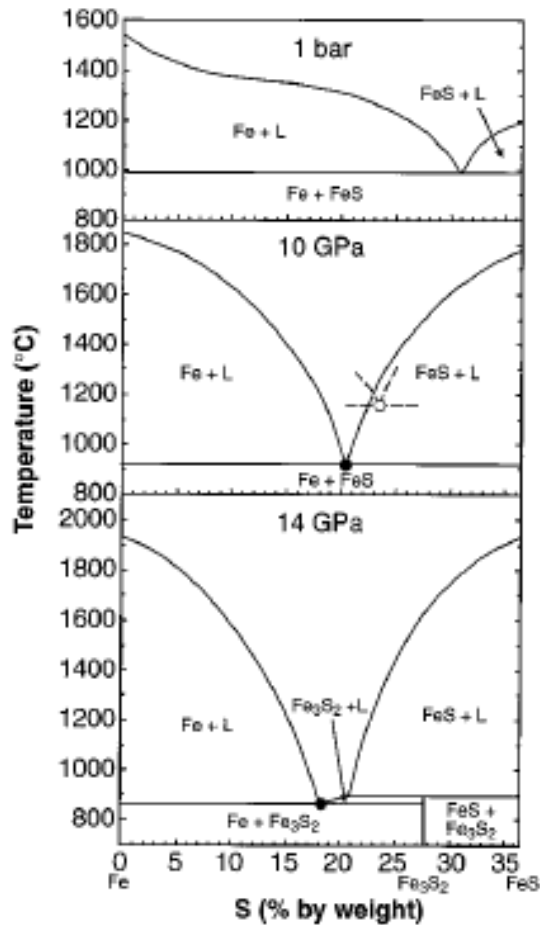


Fig. 2. Melting relations in the Fe-FeS system at pressures of (A) 1 bar, (B) 10 GPa, and (C) 14 GPa. An intermediate compound with composition Fe_3S_2 forms at pressures >14 GPa. The eutectic points at 10 and 14 GPa were determined in this study (solid circles). The eutectic point determined by Usselman (2) at 10 GPa is also shown (empty circle) for comparison. L, liquid.

Ni partitioning into Earth's mantle

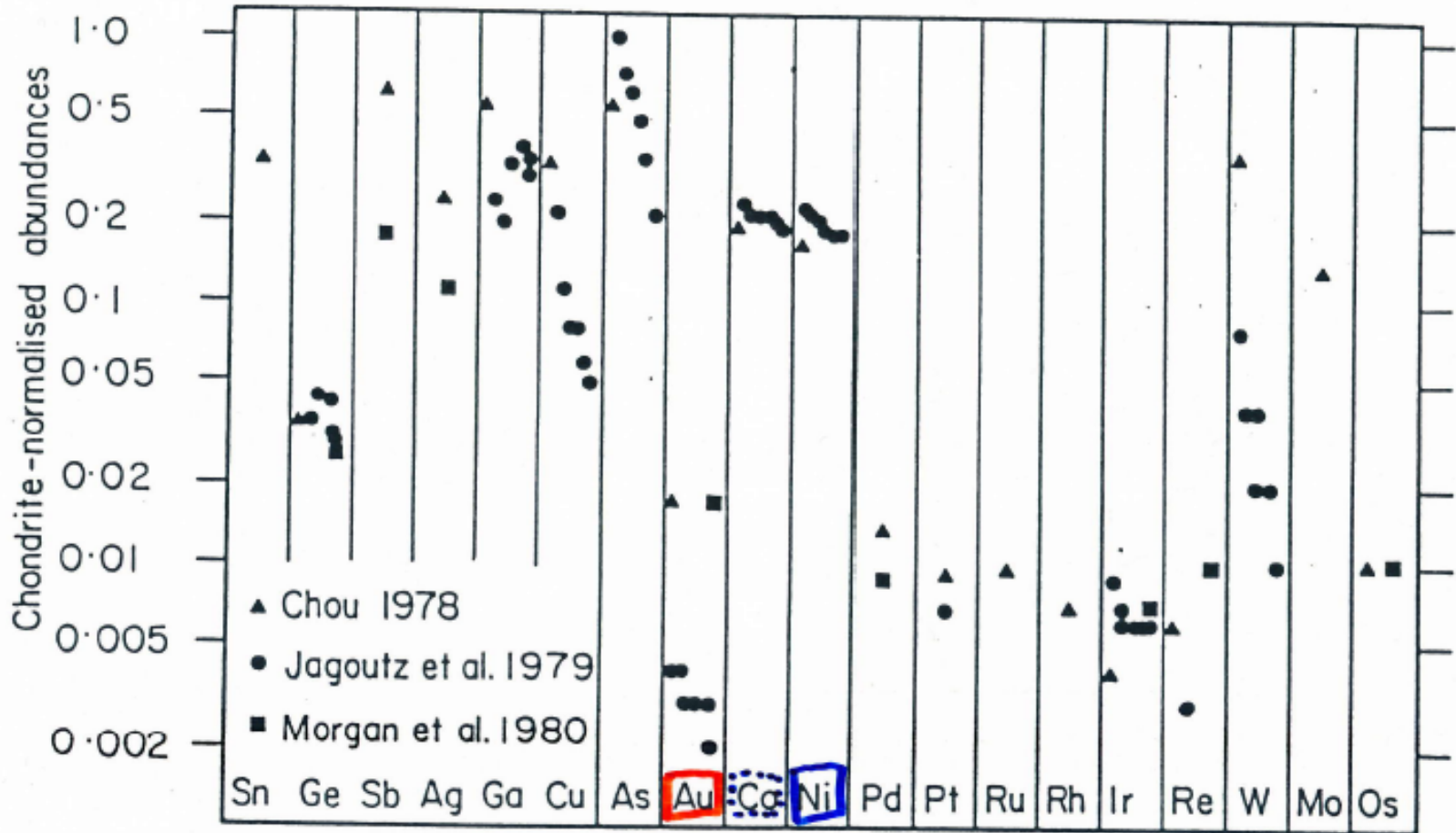
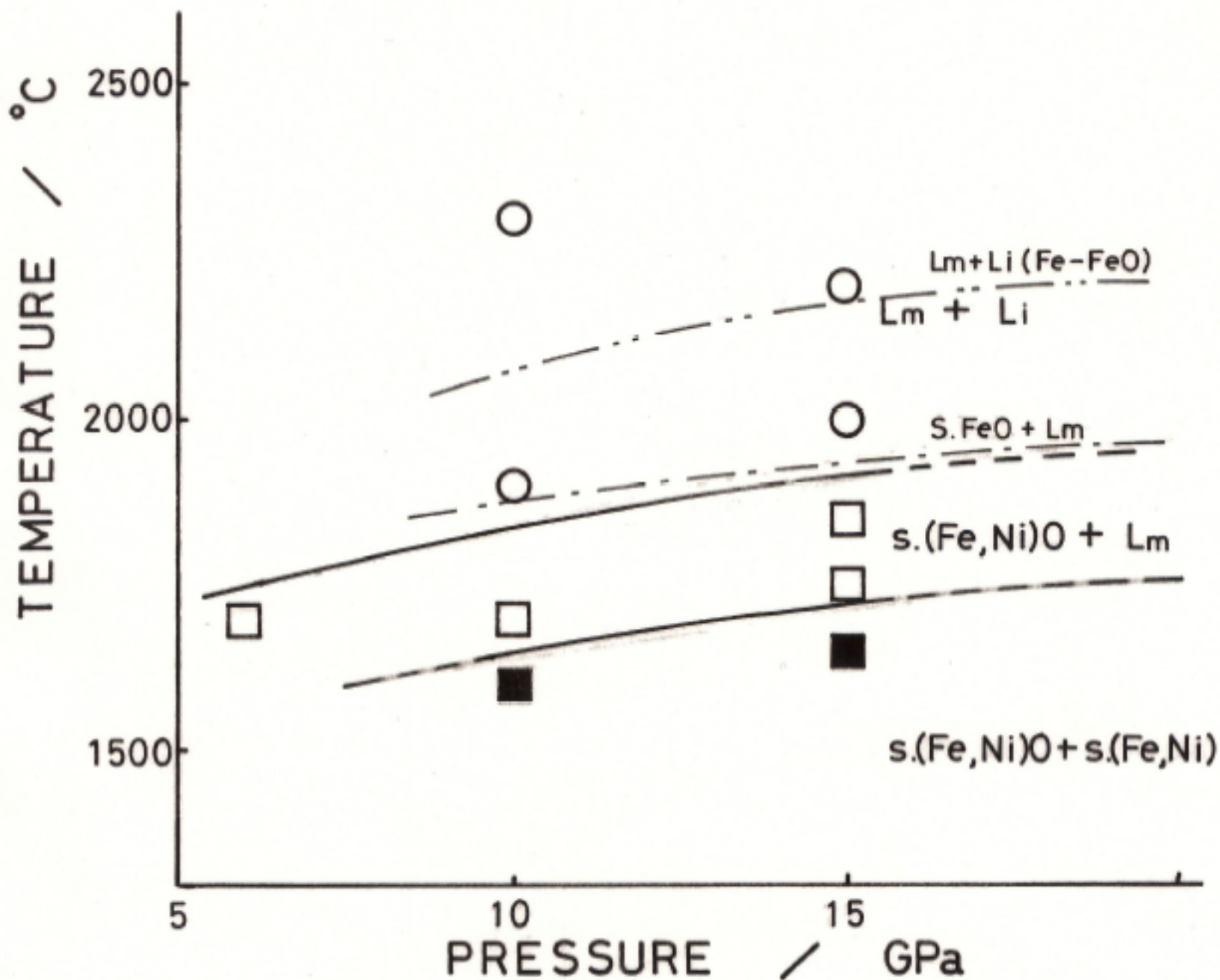
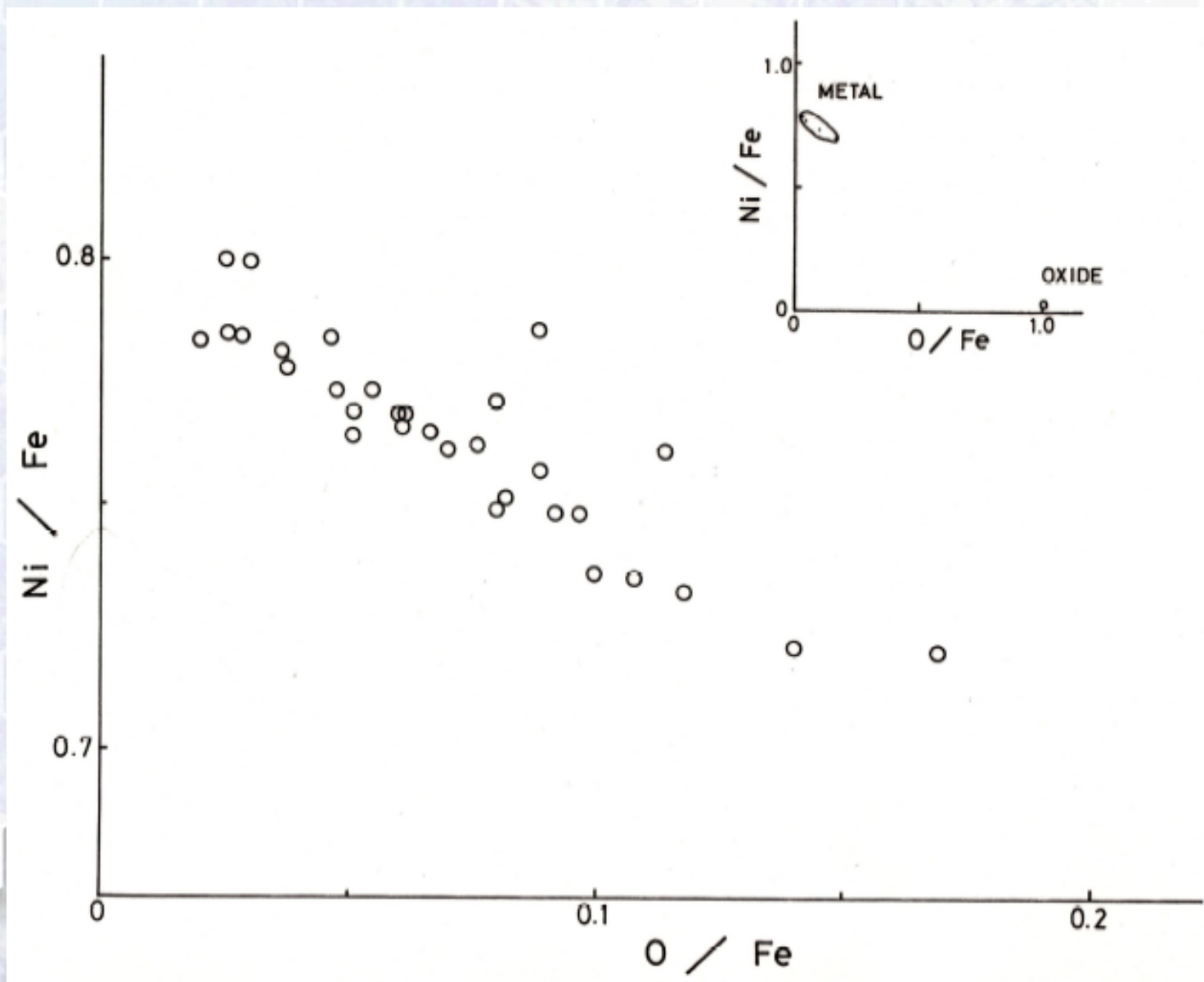


Fig. 2. Abundances of siderophile elements in the upper mantle normalized to CI chondrites displayed, from right to left, in terms of increasing volatility.

Fe-Ni-O



Ni partitioning



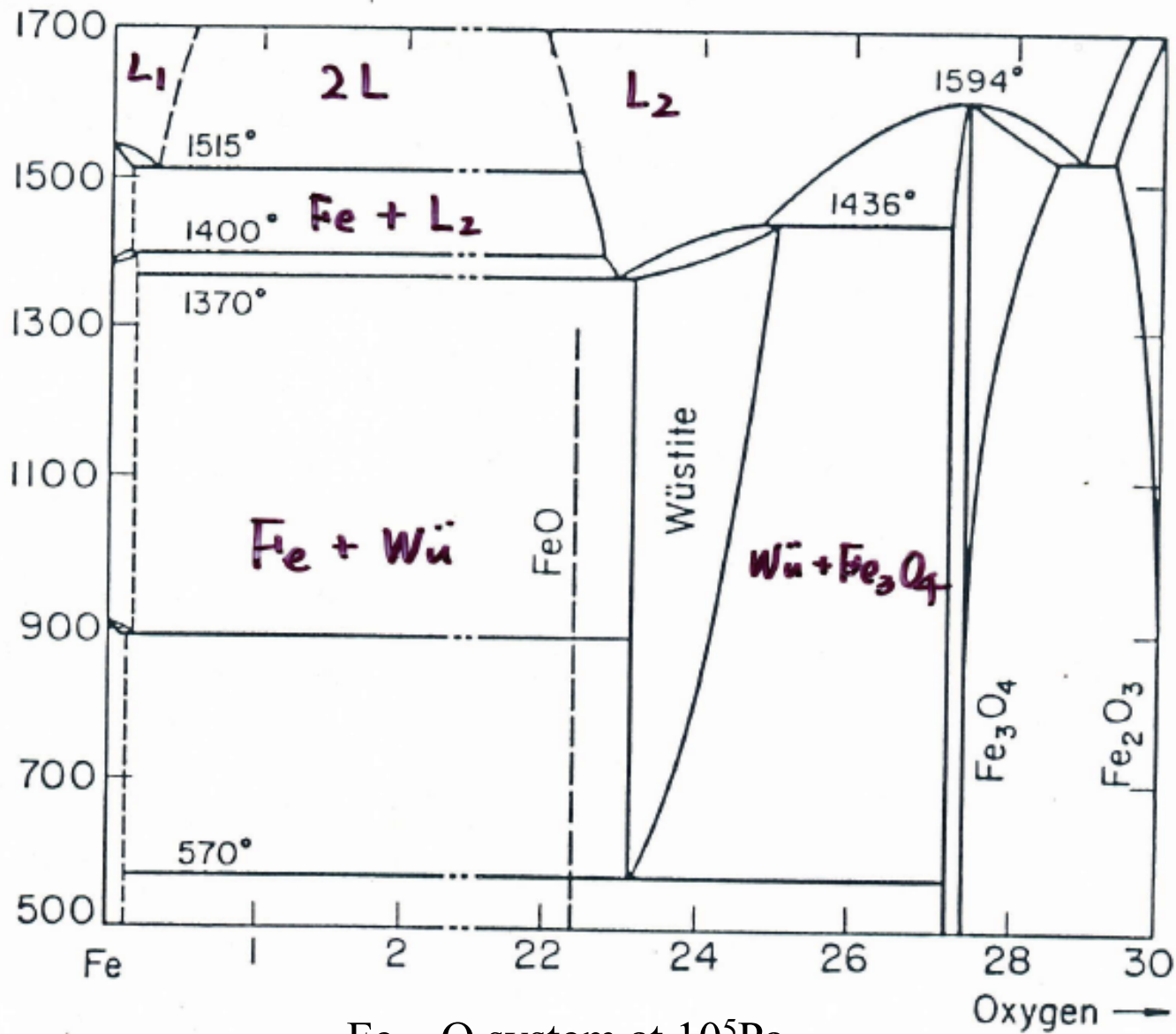
Pressure effect on Ni partitioning

Fe - Ni - O , 1700 °C

	6 GPa	10 GPa	15 GPa
O (mol%) in Lm	0.13	2.11	3.92
K	0.010	0.026	0.033

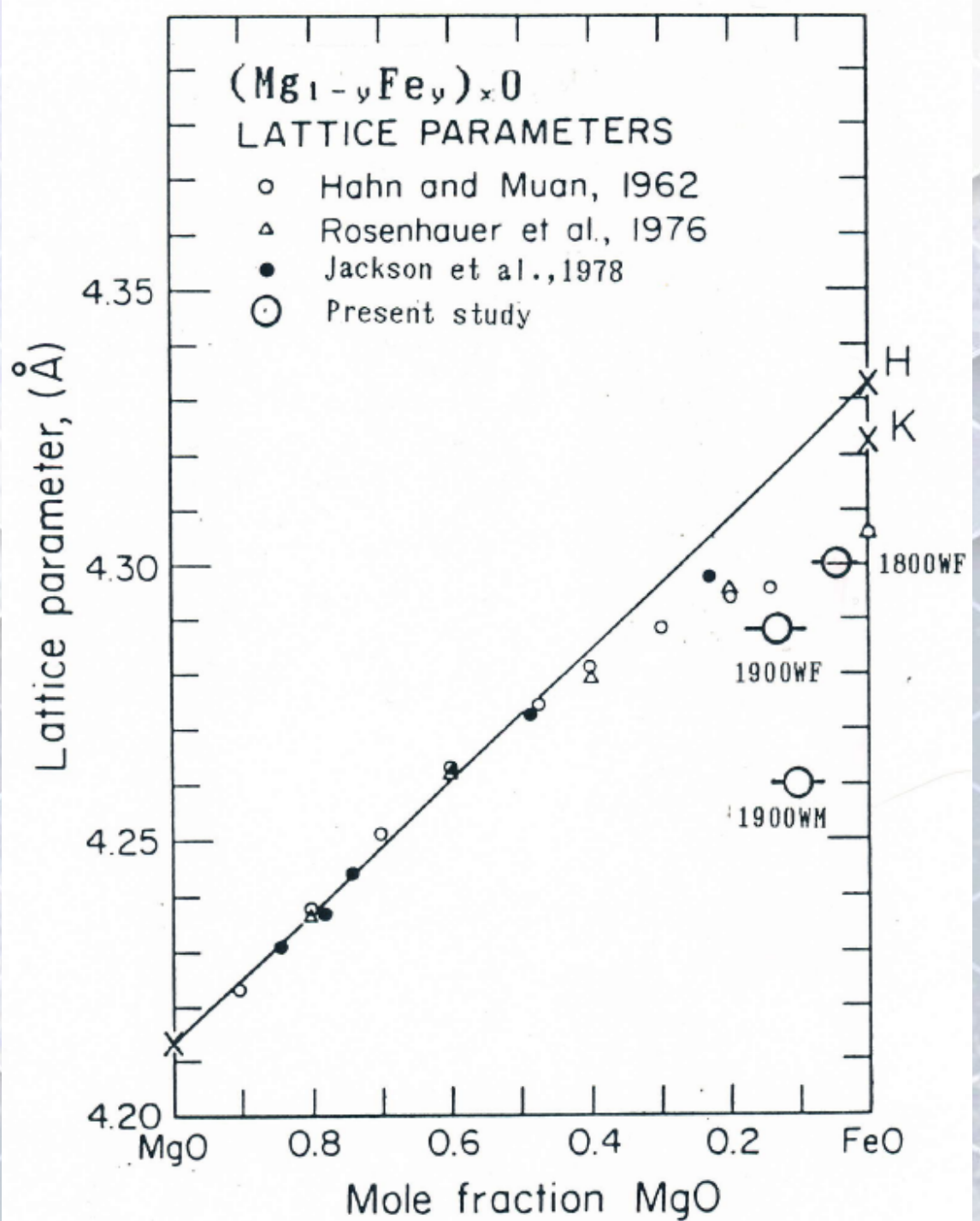
$$K = \frac{X_{\text{Ni}}^{\text{oxide}} / X_{\text{Fe}}^{\text{oxide}}}{X_{\text{Ni}}^{\text{metal}} / X_{\text{Fe}}^{\text{metal}}}$$

Pressure Effects on Stoichiometry of Fe_{1-x}O (Wüstite)



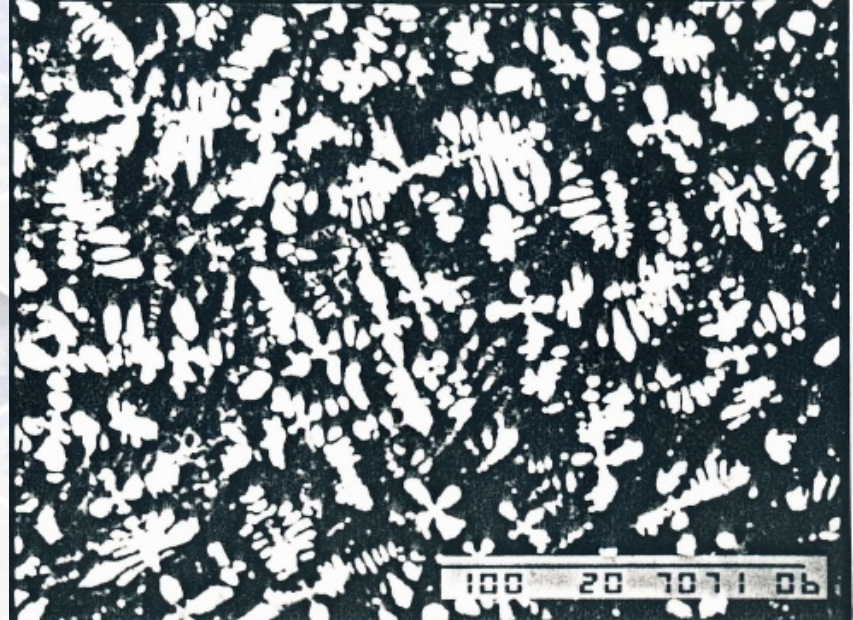
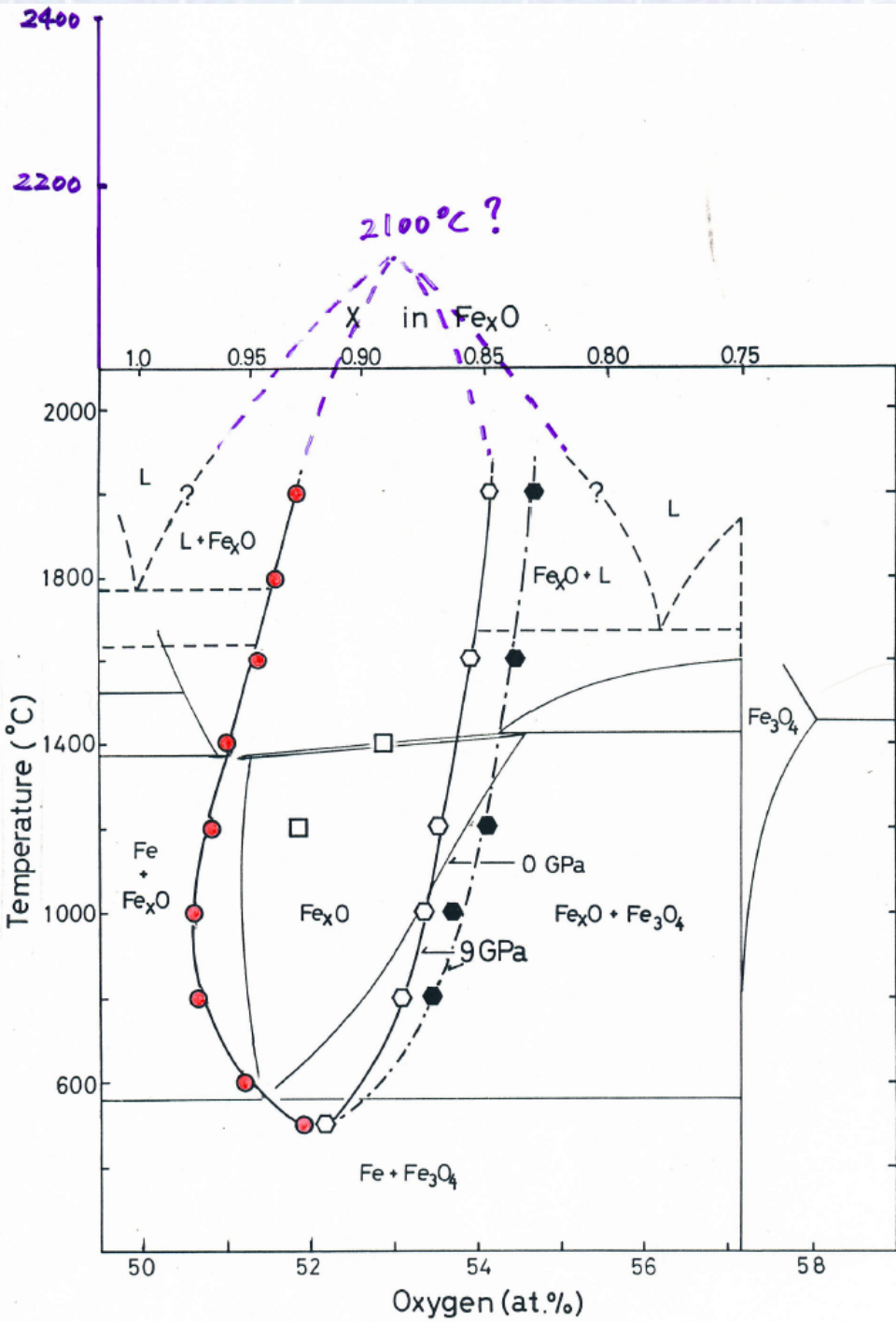
Fe - O system at 10^5 Pa

Lattice Parameters of Magnesiowüstite $(\text{Mg}_{1-y}\text{Fe}_y)_x\text{O}$

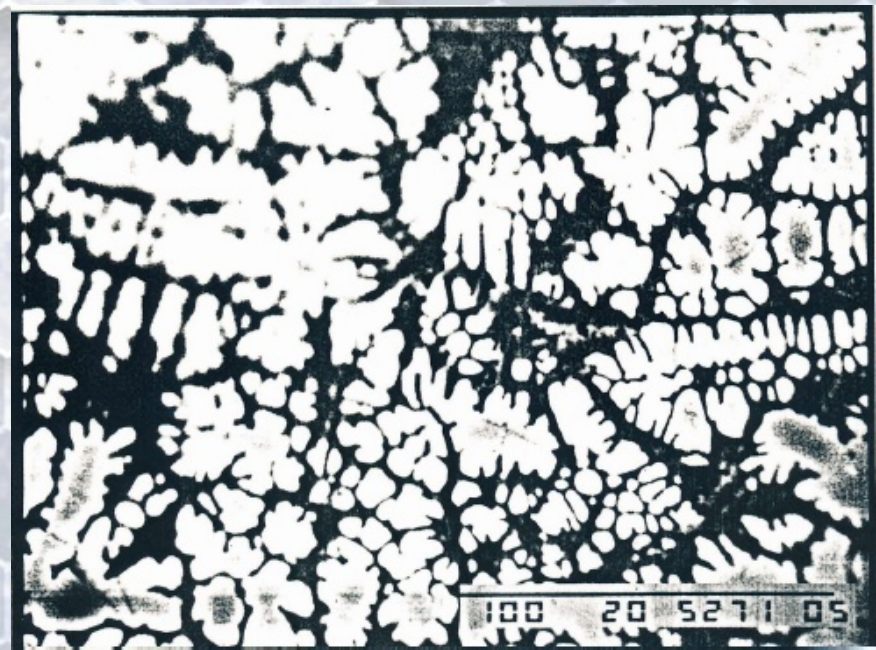


Experimental Results

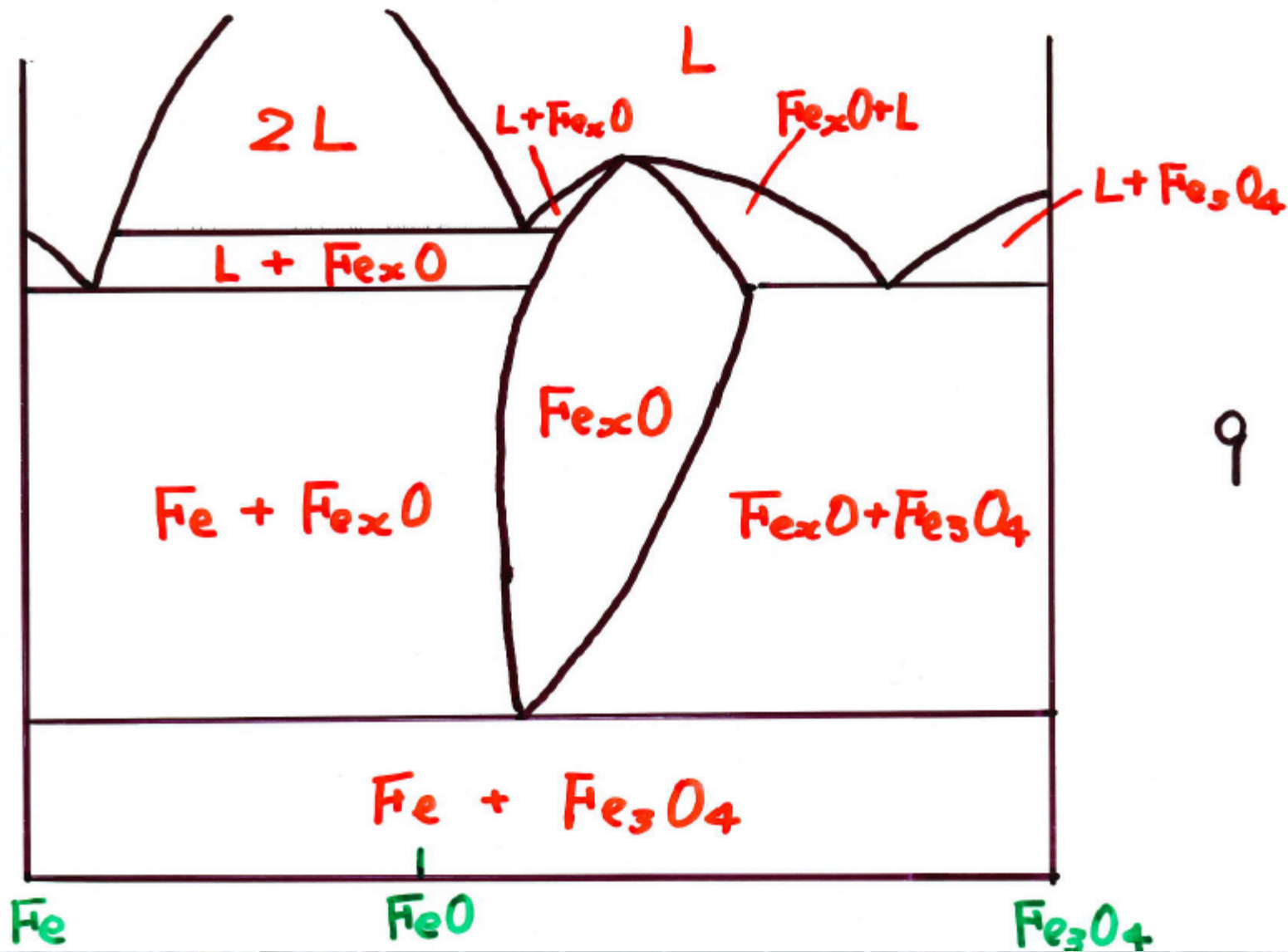
<u>P(GPa)</u>	<u>T(°C)</u>	<u>x in Fe_xO</u>	<u>Run products</u>
Starting material; Fe _x O + Fe			
9	500	0.93	Fe _x O + Fe
9	600	0.96	Fe _x O + Fe
9	1600	0.95	Fe _x O + Fe
9	1800	0.94(0.93)	<u>MW(MgO~0.05)+2L</u>
9	1900	0.93(0.90)	<u>MW(MgO~0.15)+2L</u>
15	600	0.94	Fe _x O + Fe
20	600	0.96	Fe _x O + Fe
Starting material; Fe _x O + Fe ₃ O ₄			
9	500	0.92	Fe _x O + Fe ₃ O ₄
9	600	0.88(0.87)	Fe _x O + Fe ₃ O ₄
9	1600	0.86(0.84)	Fe _x O + Fe ₃ O ₄
9	1900	0.85(0.83)	Fe _x O + L.
15	600	0.87(0.86)	Fe _x O + Fe ₃ O ₄
20	600	0.88(0.87)	Fe _x O + Fe ₃ O ₄
MW; (Mg, Fe)O			



9 GPa, 2400°C

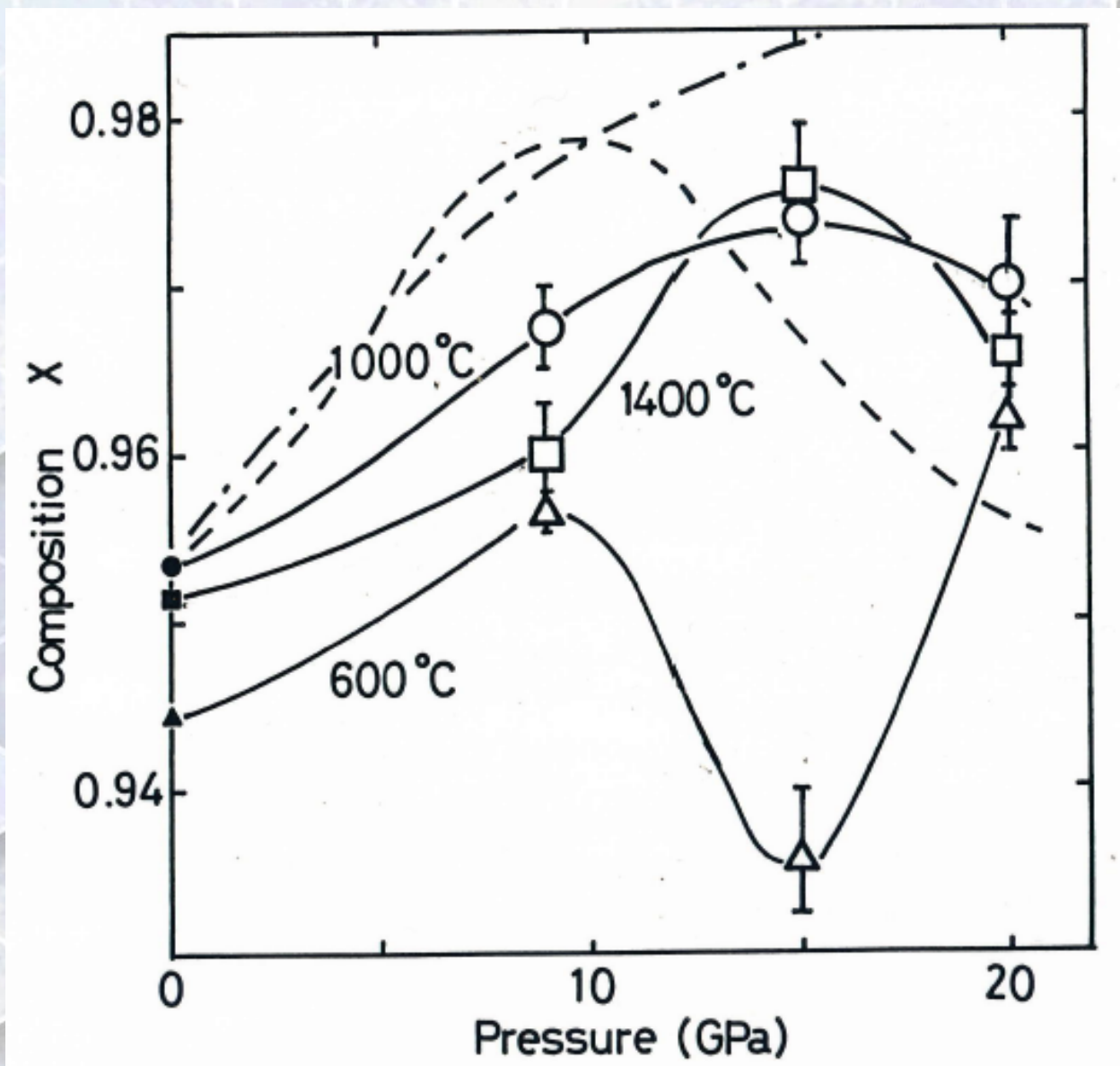


9 GPa, 2100°C



9 GP

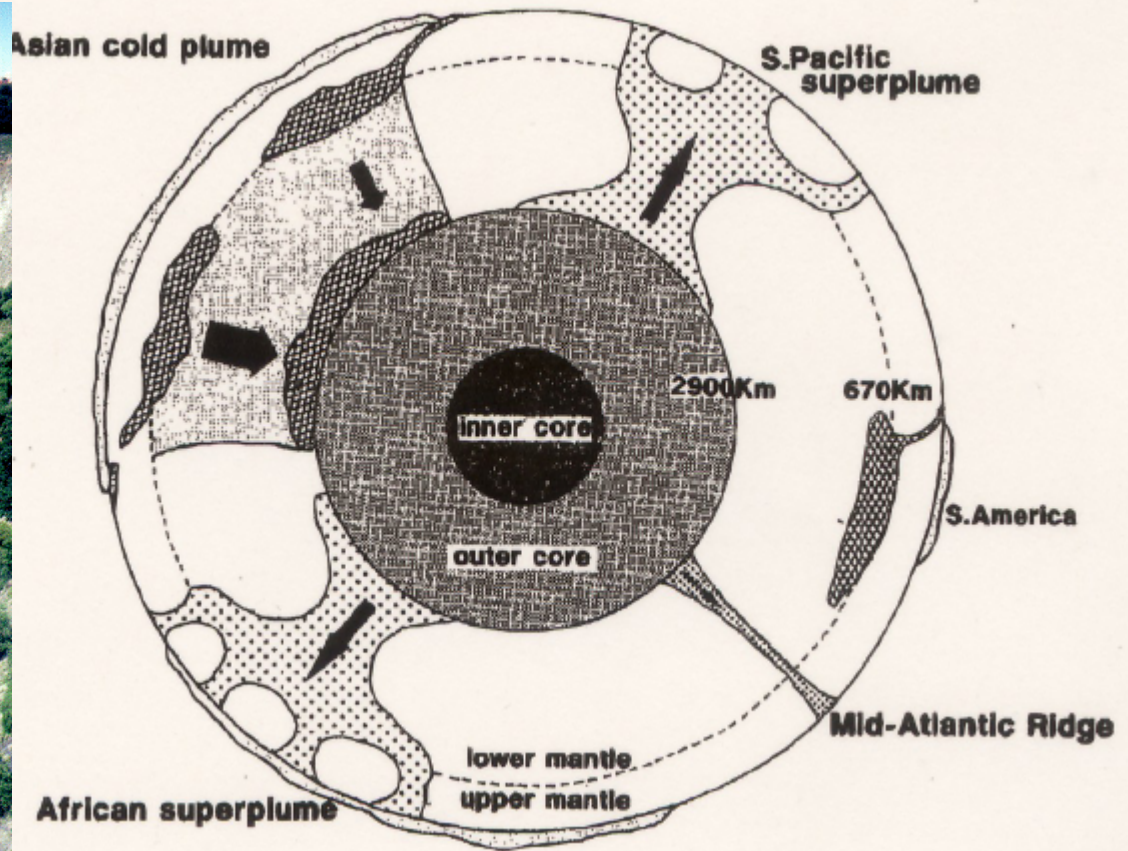
Summary



Search of extruded rocks from the Earth's lower crust and mantle



**Kimberlite Pipe
Big Hole, South Africa**



Super Plume, Maruyama 1994

Summary

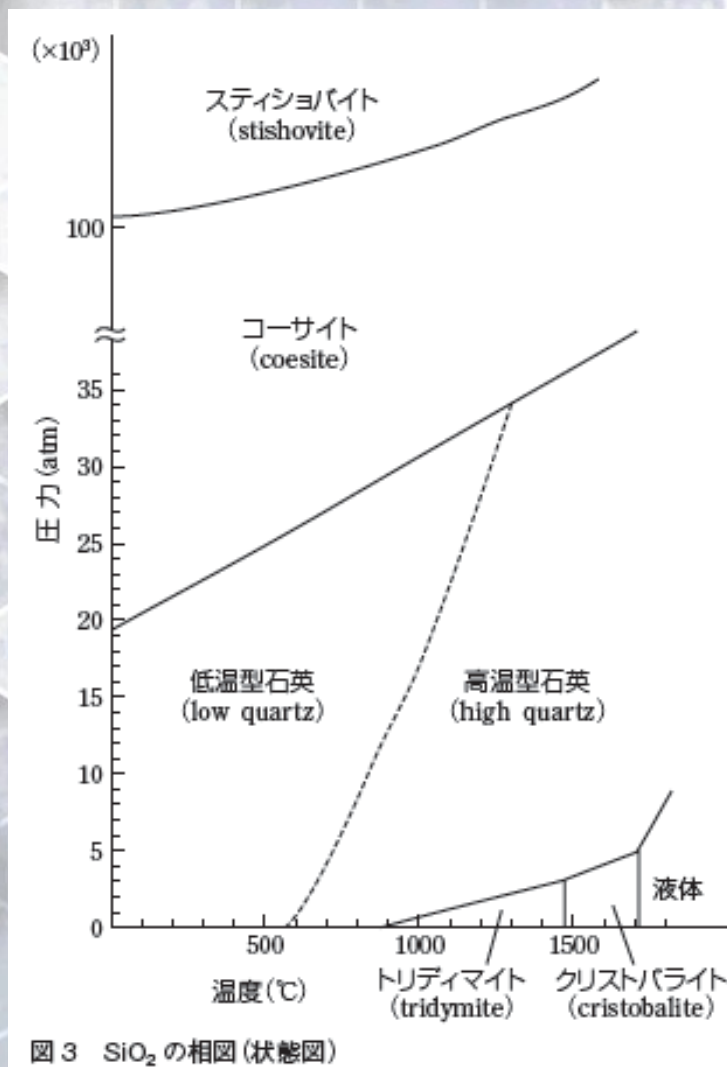
- Oxygen as the possible lightening element was examined by high P and T experiments
- Oxygen and sulfur lower the melting temperature with definite range: 800°C at 20 GPa
- Chemical corrosion enhance possibly separation process between mantle and core.

?Lightening elements

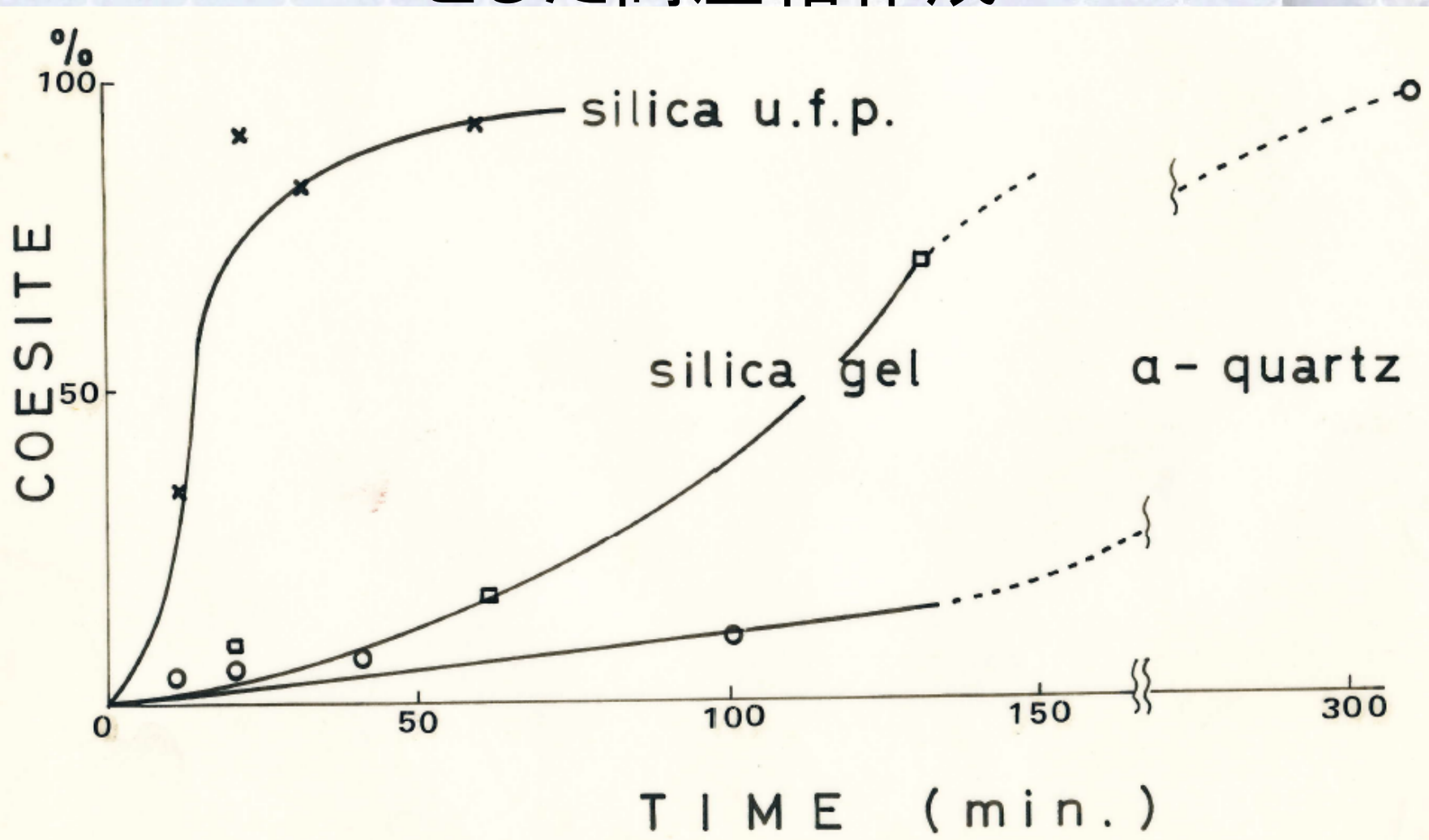
?Stoichiometry, ?Superlattice

超微粒子 SiO_2 を用いた高压相 coesiteの合成実験

- Amorphous SiO_2 超微粒子(平均粒径6nm)の合成
- 超微粒子の活性を利用して短時間で高压相鉱物 coesiteを生成

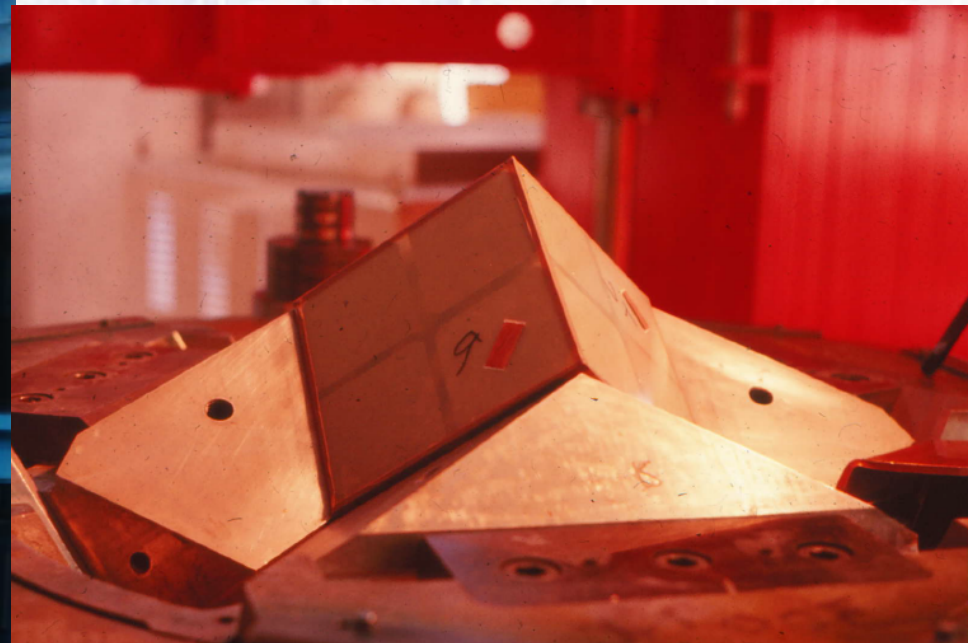


超微粒子、シリカゲル、石英を出発試料 とした高压相作成

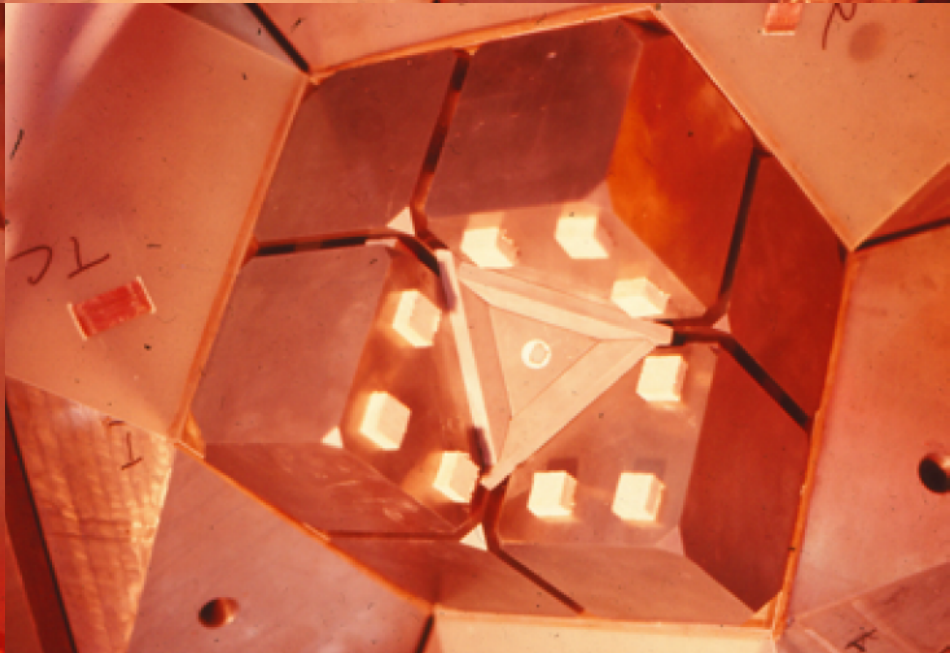
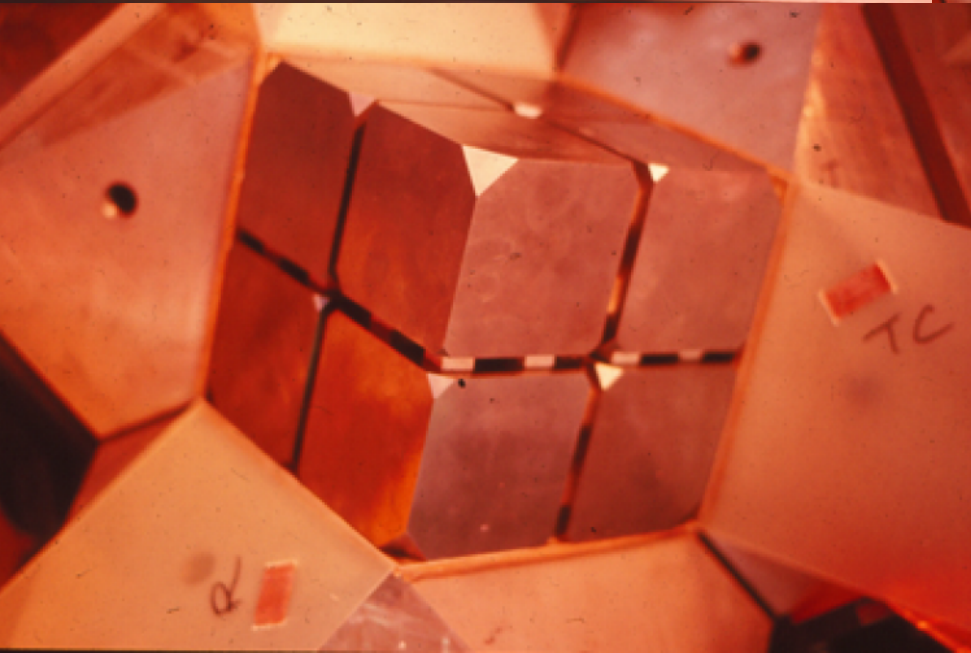
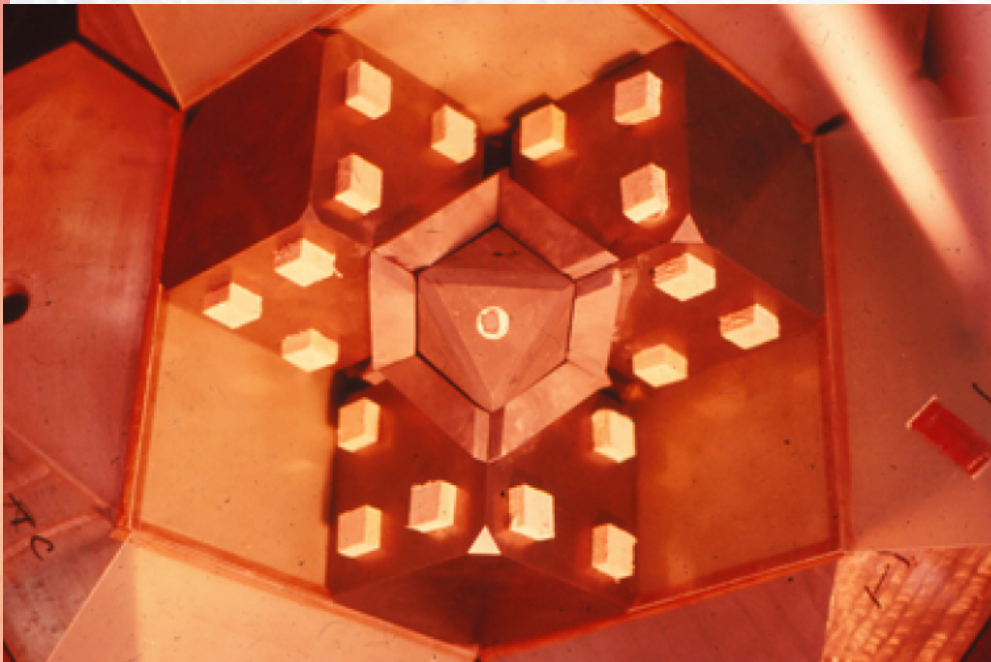
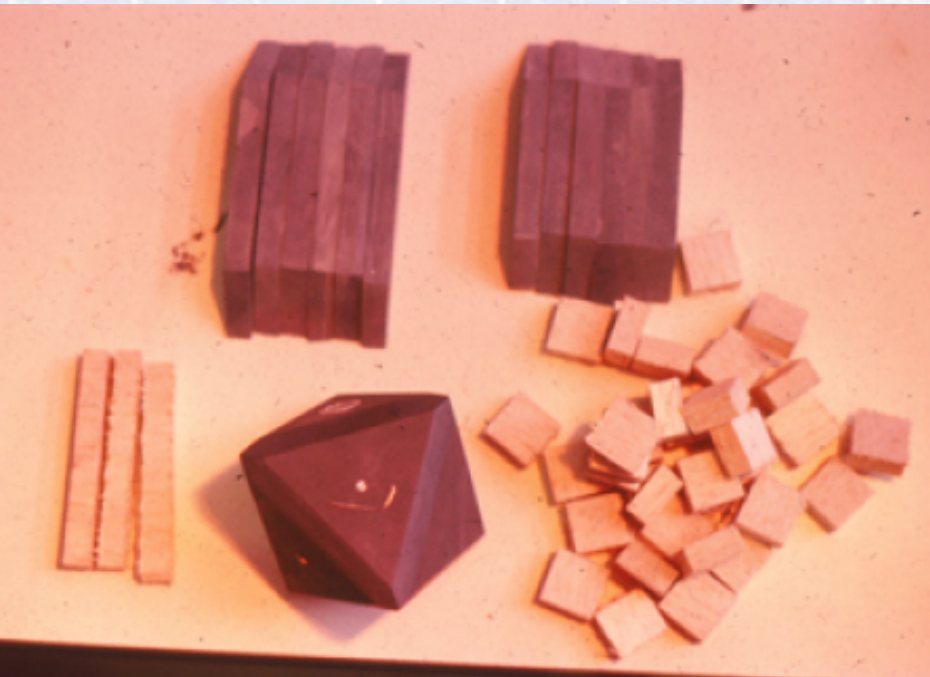


大型超高圧力発生設備の設置

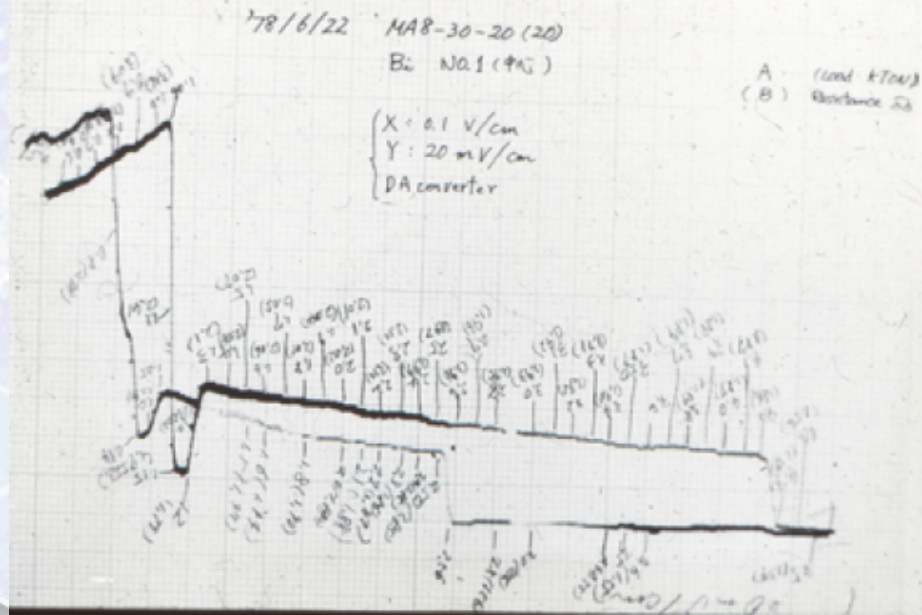
- 直径2mのシリンダヘッドに最大1万トン荷重をかけられる世界でも有数の高圧プレスを建設
- 地球中心核の圧力350GPaをmmオーダの容積に発生する
- 大体積 1 cm^3 の超硬度物質を合成できる
- 設備維持費と維持要員が確保できる予算
- 惑星科学実験解析施設の中心設備となること



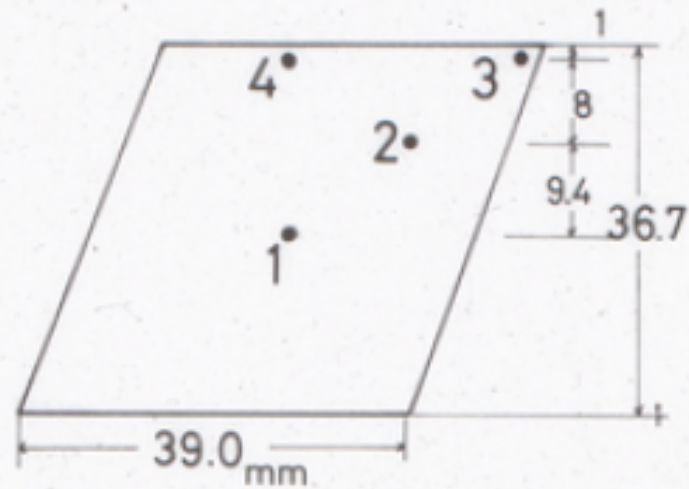
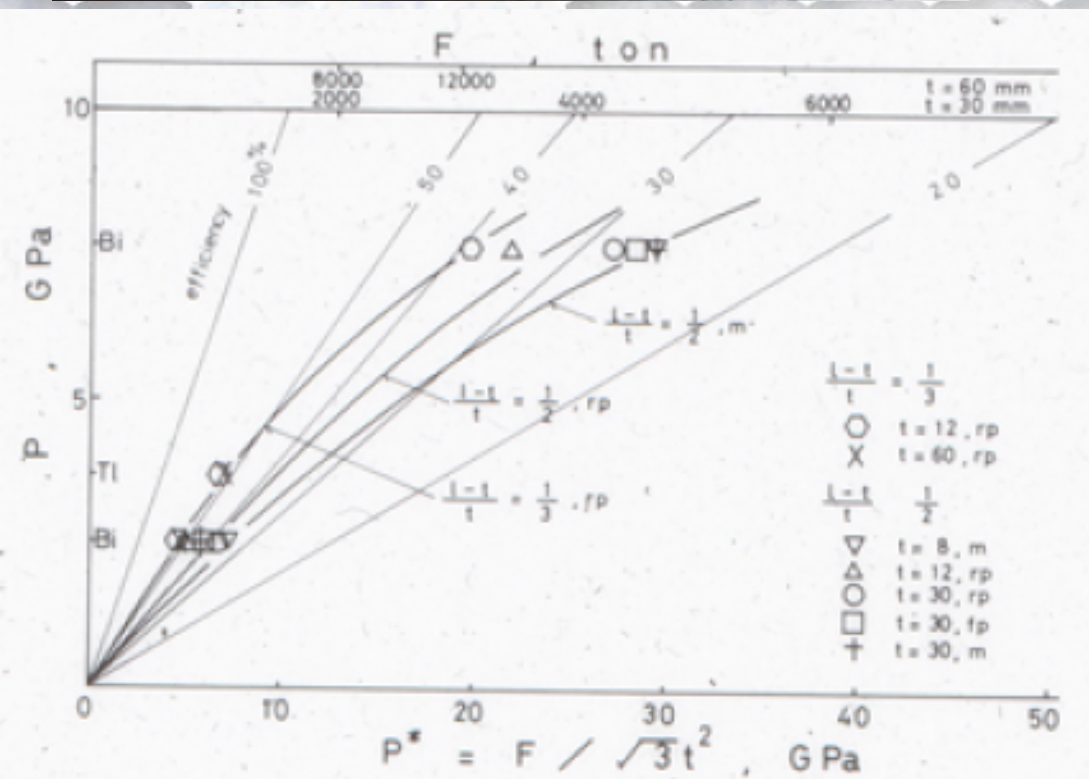
MA-8型高圧発生システムのアセンブリ



压力発生、压力分布



pm	position NO.	F, ton	
		Bi I-II	Bi III-V
rp	1	1100	4200
	2	900	3600
	3	700	3600
	4	800	3650
m	1	850	4500
	3	650	3700



大型プレスによる超硬材料の生成



(BOTCHANにより合成されたヒメダイヤ)

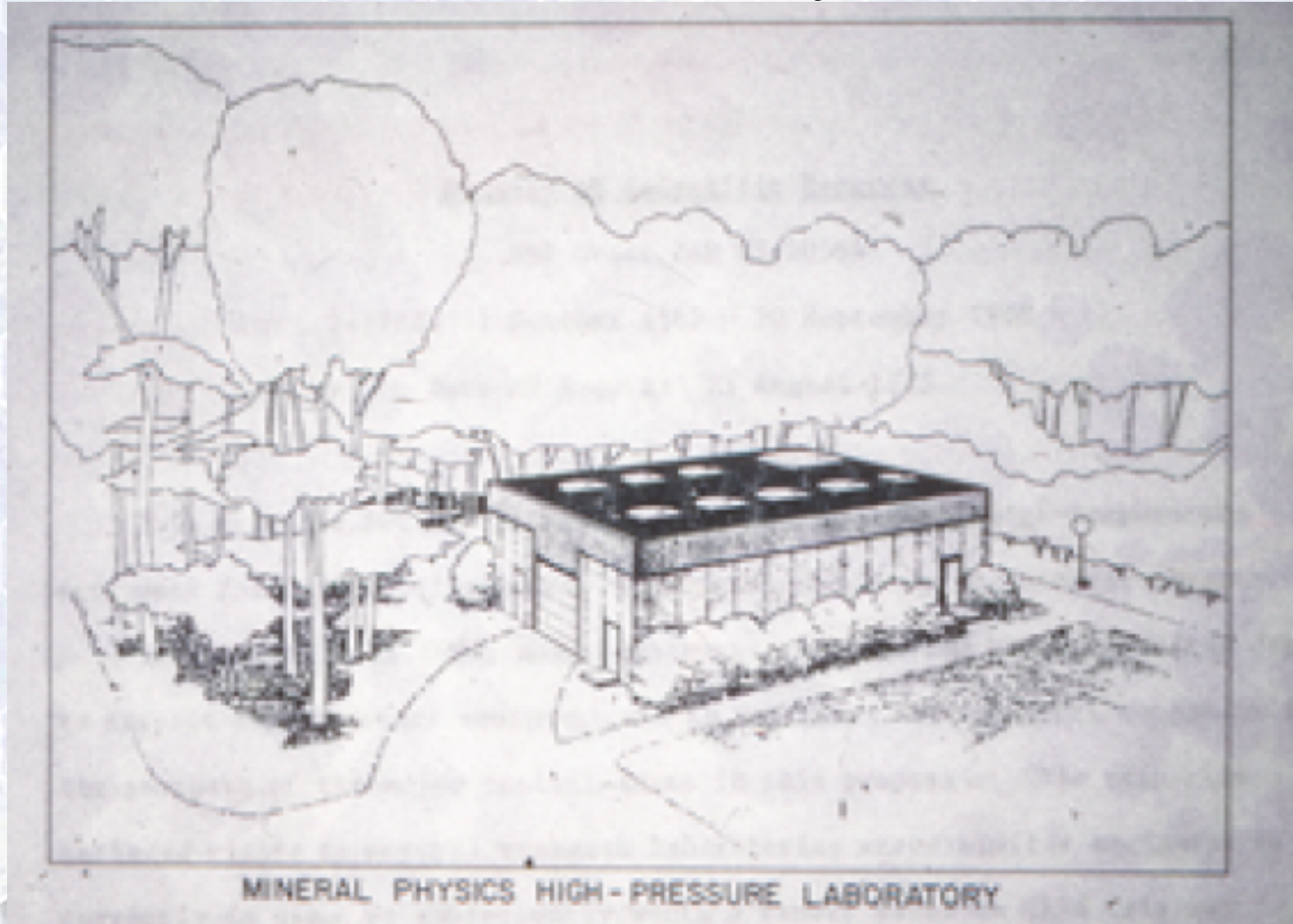


愛媛大学入船教授らによる

高圧力発生技術の輸出

- 従来DAC (Diamond Anvil Cell) と衝撃圧縮中心の欧米に日本のMA (Multi Anvil) システムの輸出
 - SUNY at Stony Brook、
 - ANU、
 - U of Bayreuth
- 日本中の高圧研究者が高圧プレス^oのセットアップのため海外へ

SUNY at Stony Brook



Mineral Physics Lab. Established in 1985



SUNY people

